

# Cross-linked cyclodextrin glucanotransferase aggregates from *Bacillus lehensis* G1 for cyclodextrin production: Molecular modeling, developmental, physicochemical, kinetic and thermodynamic properties

Nashriq Jailani<sup>a</sup>, Nardiah Rizwana Jaafar<sup>a</sup>, Suhaily Suhaimi<sup>a</sup>, Mukram Mohamed Mackeen<sup>b,c</sup>, Farah Diba Abu Bakar<sup>d</sup>, Rosli Md Illias<sup>a,\*</sup>

<sup>a</sup> School of Chemical and Energy Engineering, Faculty of Engineering, Universiti Teknologi Malaysia, 81310 Skudai, Johor, Malaysia

<sup>b</sup> Department of Chemical Sciences, Faculty of Science and Technology, Universiti Kebangsaan Malaysia, 43600 Bangi, Selangor Darul Ehsan, Malaysia

<sup>c</sup> Institute of Systems Biology (INBIOSIS), Universiti Kebangsaan Malaysia, 43600 Bangi, Selangor Darul Ehsan, Malaysia

<sup>d</sup> Department of Biological Sciences and Biotechnology, Faculty of Science and Technology, Universiti Kebangsaan Malaysia, 43600 Bangi, Selangor Darul Ehsan, Malaysia

## ARTICLE INFO

### Keywords:

Cyclodextrin glucanotransferase  
Enzyme immobilization  
CLEA  
Molecular modeling

## ABSTRACT

Type of cross-linking agents influence the stability and active cross-linked enzyme aggregates (CLEA) immobilization. The information of molecular interaction between enzyme-cross linker is not well explored thus screening wide numbers of cross-linker is crucial in CLEA development. This study combined the molecular modeling and experimental optimization to investigate the influences of different cross-linking agents in developing CLEA of cyclodextrin glucanotransferase G1 (CGTase G1) for cyclodextrins (CDs) synthesis. Seven types of cross-linkers were tested and CGTase G1 cross-linked with chitosan (CS-CGTG1-CLEA) displayed the highest activity recovery ( $84.6 \pm 0.26\%$ ), aligning with its highest binding affinity, radius of gyration and flexibility through *in-silico* analysis towards CGTase G1. CS-CGTG1-CLEA was characterized and showed a longer half-life ( $30.06 \pm 1.51$  min) and retained a greater thermal stability ( $52.73 \pm 0.93\%$ ) after 30 min incubation at optimal conditions compared to free enzyme ( $10.30 \pm 1.34$  min and  $5.51 \pm 2.10\%$  respectively). CS-CGTG1-CLEA improved CDs production by 33% and yielded cumulative of 52.62 g/L CDs after five cycles for 2 h of reaction. This study reveals that abundant of hydroxyl group on chitosan interacted with CGTase G1 surface amino acid residues to form strong and stable CLEA thus can be a promising biocatalyst in CDs production.

## 1. Introduction

Cyclodextrin glucanotransferase (CGTase) is an industrial enzyme produced primarily by bacteria of the genus *Bacillus* [1]. This unique enzyme can synthesize the cyclic  $\alpha$ -1,4-glucan from starch with 6, 7 and 8 degrees of polymerization known as  $\alpha$ -,  $\beta$ - and  $\gamma$ -cyclodextrin [1,2]. Cyclodextrins (CDs) have hydrophobic central cavities that can incorporate various inorganic and organic compounds, forming inclusion complexes [3,4] that can widely be exploited in pharmaceutical [5], foods [6], medicine [7], textile [8] and cosmetic industries [9]. As a result of its high soluble properties, CDs have become increasingly popular thereby increasing the need for more efficient catalysts in the production of CDs.

Although free CGTase appears to have diverse biotechnological

potential, it has several disadvantages in terms of industrial scale applications, including low stability under process conditions, inhibition of the enzyme's activity, and non-reusability, making their applications costly. High thermostability of CGTase to withstand harsh industrial conditions such as extreme pHs and elevated temperatures is much preferable where the desired catalyst can be modified and constructed through enzyme immobilization [10]. Immobilized enzymes have been demonstrated to have a number of promising characteristics, including high thermal stability, reusability of the catalyst, ability to catalyze reactions involving unnatural substrates, enhanced enantioselectivity and the ability to be separated from products easily [11]. The modification of enzymes through different immobilization strategies is considered to be the most straightforward, cost-effective and practical method in green biotechnology, enabling the reuse of CGTase, facile recovery, longer

\* Corresponding author.

E-mail address: [r-rosli@utm.my](mailto:r-rosli@utm.my) (R.M. Illias).

<https://doi.org/10.1016/j.ijbiomac.2022.05.170>

Received 4 January 2022; Received in revised form 14 May 2022; Accepted 24 May 2022

Available online 27 May 2022

0141-8130/© 2022 Elsevier B.V. All rights reserved.

half-lives, stabilized enzyme activity and structure, in addition reduction in the cost of CDs production [10,12].

Several immobilizations strategies of CGTase on different solid supports have been applied including covalent bonding to glutaraldehyde pre-activated silica [13], entrapment into alginate-gelatin mixed gel beads [14], and adsorption into controlled pore silica [15]. An extensive smart chemistry of enzyme immobilization using various support matrices has been reviewed recently showed that it is crucial to know the structural and functional properties of enzyme surfaces and support matrices for efficient immobilization [16]. With regard to enzyme immobilization applications, silica has been the most extensively studied mesoporous material, offering a wide range of properties such as increased surface area, thermal and mechanical stability, ease of handling, a high flow rate capability, and non-toxic properties [16,17]. In recent years, there has been significant research into biocatalysts at the nanoscale, which has greatly contributed to the development of unique nanoscale carrier matrices for the immobilization of enzymes. Nanobiocatalyst offer a significant potential for improved catalytic characteristics for use in multipurpose bioprocessing applications. A robust nanocarriers to design nanobiocatalyst has been reviewed by Bilal et al. [18] that includes the prospective of carbon, metal nanoparticle/nanocomposites, polymer and silica-based for enzyme immobilizations. The precise assembly of enzymes and nanostructures provides exciting advantages, including improved recyclability, activity, and stability through novel nano-surroundings for enzymes designed to maximize the catalytic efficiency [19]. However, a serious downside of carrier-bound enzyme immobilization is that they have low productivities and the cost contribution of the carrier is often considerably higher than free enzymes [20]. Moreover, developing nanobiocatalysts for industrial bioprocessing applications utilizing multi-enzyme immobilization remains a challenge, in addition, due to its small size, downstream processing is highly complex after the reaction [18,19].

Recently, a versatile carrier-free immobilization technique known as cross-linked enzyme aggregates (CLEA) has been gaining popularity. CLEA are less expensive biocatalysts than enzymes immobilized on solid support due to the absence of carriers, higher mass loadings, high stability under extreme operating conditions, easy recovery, separation, and reusability, and the fact that no extensive enzyme purification is required [20]. CLEA are the physical formation of enzyme aggregates by precipitating agents followed by consequent chemical cross-linking by the cross-linker [20]. While CLEA development appears as a straightforward immobilization strategy and is broadly applicable, the production of CLEA continues to be challenging as several optimizations are needed since every enzyme is a different molecule. It is necessary to establish a precise protocol for aggregation and cross-linking for each respective enzyme to produce stable and active CLEA [20]. Different precipitating agents results in different conformations of enzyme aggregates, which strongly influences the selectivity of CLEA [21]. For application in industrial processes where recovery operations such as filtration and centrifugation are needed, CLEA particle size which typically varies between 0.1 and 200  $\mu\text{m}$  is a key aspect to be considered as it directly impacts mass transfer limitations and filterability [20,21]. However, increase in size particle will promote mass transfer limitations with the consequent reduction in its overall activity. Amount of enzyme, type of cross-linker and concentration of the cross-linker are among the factors that play a major role in determining the CLEA particle size [20,21]. These parameters can both have an impact on the final result of the biocatalyst.

In preparation of CLEA, the type of cross-linker is one of the several contributing factors affecting the CLEA activity recovery. Glutaraldehyde (GA), a bifunctional cross-linker is most commonly used for the preparation of CLEA [22]. It has been used for protein cross-linking for decades because it is inexpensive and readily available in commercial quantities [23]. Even so, there may be problems with crosslinking using GA in some cases, particularly when the enzyme has few lysine residues on its surface which may reduce its cross-linking efficiency [20,23].

Previously, CGTase from *Thermoanaerobacter* sp. [24] and *Komagataella phaffii* [25] has been cross-linked using glutaraldehyde. These CLEAs were reported to maintain a very low activity recovery (10% and 4.6%, respectively). A few studies have explored several cross-linkers other than GA and found that cross-linkers such as p-benzoquinone for lipase-CLEA [26], L-lysine for the preparation of biocompatible peroxidase and urease-CLEA [27], pectin for glucoamylase-CLEA and chitosan for maltogenic amylase-CLEA [28] produced higher activity compared to GA. Based on these findings, it can be hypothesized that the formation of strong interactions and hence stable CLEA is concomitant to the association between the nature of cross-linker chemistries and the composition of enzyme surface amino acid residues..

The screening of the crosslinkers can be a labour-intensive step in developing CLEA. Herein, computational molecular docking and molecular dynamic simulations (MD) techniques are used to examine and screen the cross-linkers for the purpose of developing CGTase-CLEA and the *in-silico* results are validated experimentally. Molecular docking techniques aim to predict the best matching binding mode of a ligand to a macromolecular protein [29] while MD simulation is a computational technique which simulates the dynamic behavior of molecular systems as function of time [30]. With the emergence of high-end computational power, MD simulations can provide precise information on the motions and flexibility of protein, which contributes to the interaction dynamics of protein–ligand complexes [31]. MD simulations have been applied to investigate the interaction of immobilized enzyme onto solid support. Interaction details between enzymes such as D-psicose 3-epimerase [32] and chymotrypsin [33] with graphene oxide and interactions of single-walled carbon nanotubes with lysozyme [34] and hydrolases [35] have been shown by MD simulations. However, investigation of the molecular interaction of a protein with a cross-linker using MD simulation, particularly in carrier-free CLEA immobilization, has yet to be well studied and explored.

Thus, the aim of this study is to explore the influence of cross-linkers with different functional groups, their binding energy and the molecular interaction of surface amino acid residues of CGTase from *Bacillus* sp. G1 in cross-linking using combination of *in-silico* analysis and experimental screening to produce the most active CGTase G1-CLEA. To the best of our knowledge, this is the first report which integrates molecular docking and molecular dynamic simulations with experimental work for screening of cross-linkers in the development of CLEA. Seven different cross-linkers were studied, including benzoquinone, chitosan, ethylene glycol-bis (succinic acid *N*-hydroxysuccinimide ester) (EG-NHS), glutaraldehyde, dialdehyde-starch, pectin, and polyethylene glycol 8000 (PEG8000) with CGTase G1. In this study, *in-silico* and experimental results were corroborated, offering insight that computational tools can provide in reducing the time spent on the screening process as well as in reducing the costs and time spent on developing CLEAs. A number of parameters, including the type of precipitant, the crosslinking agent concentration, and the crosslinking time, were optimized to develop the CGTase G1-CLEA. The CLEA were characterized for their optimum pH and temperature, functional group analysis, thermal and pH stability, CDs production, and operational stability. The kinetic and thermodynamics parameters of immobilized CGTase G1 were evaluated. CGTase G1-CLEA, generated as a result of both computational and experimental work here, showed higher activity recovery, improved thermostability and CDs production compared to free enzyme and previous CLEA suggests that this immobilization strategy is proven to be able to generate promising biocatalysts for producing CDs from starch.

## 2. Methodology

### 2.1. Computational analysis

#### 2.1.1. Homology modeling and structure refinement

Homology modeling was used to construct the 3-Dimensional (3D) structure of CGTase from *Bacillus* sp. G1 (CGTase G1, Gene Bank

Accession number: AY770576). CGTase from *Bacillus stearothermophiles* (PDB ID: 1CYG) was chosen as the template due to its lowest E value, sequence identity and sequence similarity (>30%) that allows the generation of a reliable model. [36]. Homology modeling was performed using Modeller 9.13 software, and the internal algorithm for the optimization level option for model building was set to high where the program used a thorough Gromacs version 4.6.3 molecular dynamic simulation annealing step when building the first model [37]. Hundreds of CGTase G1 models were generated and model with the lowest energy value based on molecular pdf (molpdf) and discrete optimize protein energy (DOPE) (molpdf and DOPE score of hundreds of CGTase models were listed in Supplemental Data Table S1†) was selected and evaluated by the root mean square deviation (RMSD), ERRAT and Verify3D. A model with the best scores was further optimized by gradual energy minimization in three stages. Constraints in all stages were of positional harmonic constraints of 20 kcal/mola, applied to all the back-bone atoms. The steepest descents method was set at 500 steps for the first minimization, followed by 1000 steps of the conjugate gradient method.

### 2.1.2. Docking analysis

The 3D structure of CGTase G1 was subjected to protein-ligand (linkers) docking. A .pdb file of the cross linker (glutaraldehyde, chitosan, dialdehyde starch, benzoquinone, EG-NHS, pectin and PEG8000) structure was obtained from PubChem [38]. An automated docking simulation of CGTase with cross linkers were performed using the Autodock Vina program [39]. Autodock Tools was used to generate pdbqt files of receptor and ligands from their traditional PDB files to be used in the AutoDock Vina. The .pdbqt file is an extension .pdb format of coordinate file that includes atomic partial charges. Hydrogen atoms were added to the macromolecule and partial atomic charges were calculated. A grid box with size of 40 × 40 × 40 points was used in the configuration file of the AutoDock Vina software to cover the entire CGTase G1 enzyme. The grid box was centered at the coordinate X: 55.226, Y: 56.06, Z: 60.087. The protein (receptor) atom positions were held fixed, and the torsion angle of the ligands (cross linkers) bond was rotated until the rigid docking in program AutoDock Vina for allowed the favorable docking. Other docking parameters were set as default.

### 2.1.3. Enzyme-crosslinker complex molecular dynamic (MD) simulation

The stability of the docked complexes was investigated using the Gromacs MD simulation software. Protein topology was prepared using the united-atom GROMOS96 43a2 force field, while ligand topology was prepared using the PRODRG2 server (<http://davap1.bioch.dundee.ac.uk/cgi-bin/prodrg>). Following this, a protein-ligand complex topology file was created by combining the coordinates of the protein topology and ligand topology file. The models were solvated with the 1.0 nm simple point charge (SPC) water embedded in the simulation boxes. Sodium ions were added into the system to replace SPC water molecules and neutralize the system. The simulation was performed using periodic boundary conditions (PBC) and particle mesh Ewald (PME) summation to improve electrostatic interactions [40]. Subsequently, all systems were minimized using 1000 steps to a steepest descent energy minimization. Simulations were performed at 333 K using GROMACS 4.6 package and all the resulting trajectories were analyzed using GRO-MACS utilities [37]. All systems were equilibrated for 50 ps of solute position-restrained MD. The radius of gyration, root mean square deviations (RMSDs) and root means square fluctuations (RMSFs) were calculated over the 1000 ps production simulation for all backbone atoms and Ca of 671 residues respectively. In addition, hydrogen bond changes between ligand and protein, hydrophobic strength between ligand and protein were also analyzed by Gromacs.

### 2.1.4. Analysis of the structure

The pdb file of the crystal structure of CGTase from *Bacillus stearothermophiles* (1CYG) was obtained from the PDB database and was used as the reference for structural comparison against CGTase G1. All

graphical presentations of the 3D models were prepared using PyMOL [41]. The 2D drawings of cross linkers (ligands) interacting with the residues in the CGTase G1 were visualized using LigPlus version 2.2.4 [42].

## 2.2. Preparation and development of CGTase G1-CLEA

### 2.2.1. Materials

All chemicals and reagents used were of analytical and molecular biological grade purchased from Merck and Sigma Aldrich unless stated otherwise. HisTrap™ HP 5 mL column containing nickel was purchased from GE Healthcare, United Kingdom.

### 2.2.2. Expression and purification of CGTase G1

The alkalophilic bacteria identified as *Bacillus* sp. G1 was isolated from local soil [43]. The CGTase gene (GenBank Accession number: AY770576) was cloned into the expression vector pET21a(+) and expressed in the host *Escherichia coli* BL21 (DE3). This vector contains the signal peptide GlcNAc-binding protein A (GAP) that directs the expression of CGTase G1 into the extracellular space [44]. The transformed cells were grown in 100 mL of Luria-Bertani (LB) broth containing 100 µg/mL ampicillin and incubated at 37 °C for 16 h. The overnight culture (10 mL) was used to inoculate 1 L of LB broth containing 100 µg/mL ampicillin and incubated at 37 °C until its OD<sub>600</sub> reached 0.7. Recombinant gene expression was induced by addition of 0.5 mM isopropyl-β-D-thiogalactopyranoside (IPTG) and further incubation at 30 °C for 24 h. After 24 h of enzyme expression, the culture was harvested and centrifuged at 1792×g for 40 min. The supernatant was collected and concentrated using a Sartoclon Slice 200 cassette with a 30 kDa cut-off. The crude extract was purified using an AKTAPrime chromatography system with a HisTrap™ HP 5 mL column. The purification was performed according to manufacturer's protocol using a binding buffer consisted of a low concentration of imidazole (20 mM Na<sub>2</sub>HPO<sub>4</sub>, 0.5 M NaCl<sub>2</sub>, 20 mM imidazole) and the elution of CGTase G1 was performed using a high concentration of imidazole containing buffer (20 mM Na<sub>2</sub>HPO<sub>4</sub>, 0.5 M NaCl<sub>2</sub> and 5 M imidazole). The buffers were adjusted to pH 7.4 and all purification steps were performed at 4 °C. Protein concentration was using Pierce BCA Protein Assay™ kit from Thermo Fisher determined according to manufacturer's protocol with BSA as the standard.

### 2.2.3. Enzymatic assay

CGTase G1 activity was quantified using a phenolphthalein assay as established by Kaneko et al. [45] with slight modifications [46]. The reaction mixture containing 1 mL of 0.04 g soluble starch (4% w/v, 0.117 M) as a substrate in 0.1 M sodium phosphate buffer (pH 6) and 100 µL of enzyme solution (soluble) or 100 µL of immobilized enzyme suspension was incubated at 60 °C for 10 min in a water bath. The reaction was stopped by adding 20 µL of 5 M NaOH (to a final concentration of 0.1 M). A volume of 0.7 mL of 0.02% (w/v) phenolphthalein in 5 mM Na<sub>2</sub>CO<sub>3</sub> was then added to the reaction mixture. After 15 min incubation at room temperature, the decrease in color intensity was measure at 550 nm using Epoch™ Microplate Spectrophotometer. The β-cyclodextrin concentration was determined from a calibration curve of β-CD ranging from 1 mg/mL to 12 mg/mL. One unit (U) of enzyme activity was defined as the amount of enzyme that produces 1 µmol β-cyclodextrin/min under the assay conditions.

### 2.2.4. Precipitant selection

A volume of 900 µL of the precipitating agent (ethanol, acetonitrile, methanol, isopropanol, tert-butanol, dimethylformamide, acetone and dimethyl sulfoxide) concentration 99.9% (v/v) was added to 100 µL enzyme solution (0.03 mg/mL) in 0.1 M sodium phosphate buffer (pH 6) to a final concentration of 90% (v/v). After continuous shaking at 200 rpm and incubation at 20 °C for 1 h, the suspension was centrifuge at 10000×g for 1 min. The precipitate was re-dispersed in 0.1 M sodium

phosphate buffer (pH 6) and its enzymatic activity and protein concentration were determined using colorimetric phenolphthalein and BCA assay methods, respectively. The precipitant was chosen based on its precipitation yield ( $P_Y$ ) in terms of activity calculated as Eq. (1):

$$P_Y = \frac{\text{Total re - dispersed activity}}{\text{Total initial activity}} \times 100 \quad (1)$$

Concentrations ranging from 70% to 90% (v/v) also was evaluated for the selected precipitant.

### 2.2.5. Cross linking method optimization using glutaraldehyde

Four methods were optimized to prepare the CLEA with the highest activity recovery and were compared. For the common CLEA preparation (Method 1, henceforth denoted as M1), after the precipitation step, glutaraldehyde (25%, v/v) was added to the physically aggregated enzymes to a final concentration of 0.005, 0.01, 0.05, 0.10, 0.15 and 0.20%. Cross linking was maintained at 20 °C for 1 h with constant shaking at 200 rpm. At the end of the reaction time, the suspension was centrifuged at 4000×g for 1 min [24]. The supernatant was decanted and the resulting CLEA were re-suspended in 0.1 M sodium phosphate buffer at pH 6 and centrifuged again. This washing step was repeated three times. The activity recovery ( $A_R$ ) of the enzyme in the CLEA and supernatant was determined as Eq. (2):

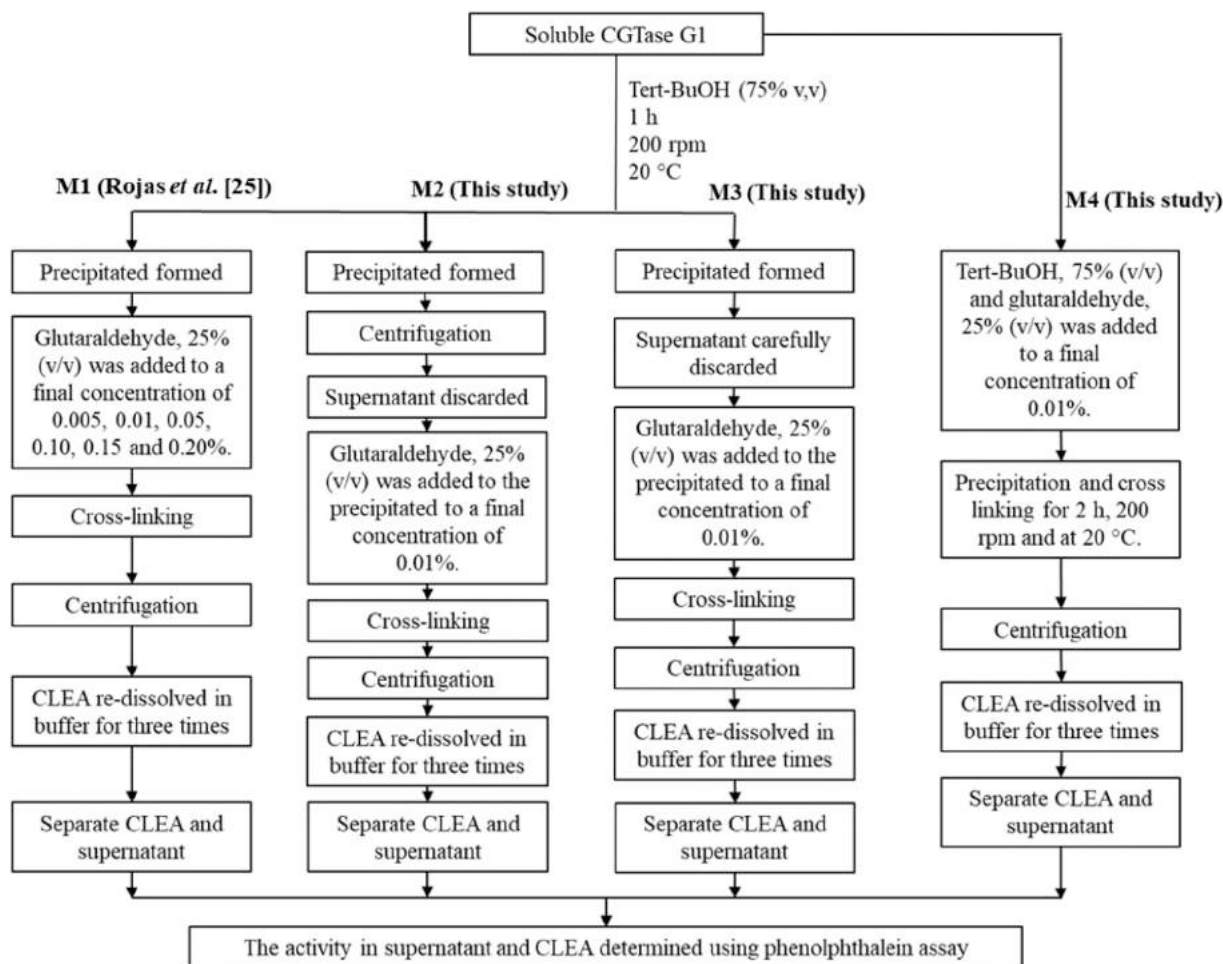
$$A_R = \frac{\text{Total activity of CLEA/supernatant}}{\text{Total initial activity}} \times 100 \quad (2)$$

For Method 2 (henceforth M2), the aggregation formed after precipitation was centrifuge at 4000 ×g for 1 min and the supernatant

(precipitating agent) was discarded. Glutaraldehyde (25%, v/v) to a final concentration of 0.01% (the highest activity recovery based on M1) was added and the cross linking continued for 1 h at 20 °C with constant shaking at 200 rpm. The washing step and activity recovery was carried out and determined as in M1. For Method 3 (M3), the aggregation formed after precipitation was left to settle at the bottom of the micro-centrifuge tube for 10 min. The supernatant (precipitating agent) was carefully removed without disrupting the aggregates, then the glutaraldehyde was added to a final concentration of 0.01%. Cross linking, washing step and activity recovery was carried out and determined as in M1. For Method 4 (M4), both aggregation and cross-linking were performed simultaneously, 900 μL of the precipitating agent (75%, v/v) with 0.01% glutaraldehyde at final concentration was added to 100 μL enzyme solution (0.03 mg/mL). The reaction was carried out for 2 h, maintained at 20 °C with constant shaking at 200 rpm. CLEA separated, washed and activity determined as describe above. Method optimizations were simplified in the Scheme 1 below.

### 2.2.6. Dialdehyde-starch (DAS) macromolecule synthesis

Dialdehyde-starch (DAS) was prepared as described by Yu et al. [47] with some modifications. Briefly, 4% (w/v) of soluble starch was dissolved in distilled water with total volume of 10 mL and mixed with 27 mL of 0.6 M sodium periodate (NaIO<sub>4</sub>) solution magnetic stirring. The pH was adjusted to 3.5 with hydrochloric acid (HCl). The mixed solution was stirred at 35 °C in the dark for 8 h. At the end of the reaction, the starch was washed three times with distilled water and anhydrous ethanol. The powdered dialdehyde starch was dried in an oven at 60 °C overnight. The percentage and concentration of dialdehyde in DAS was



Scheme 1. Optimization of cross-linking method using glutaraldehyde.

quantified using the methods reported by Veelaert et al. [48] and Tummalapalli and Gupta [49], respectively. The aldehyde content was determined to be 40% with concentration of 0.05 mmol/g.

### 2.2.7. Screening of the cross linkers

The cross-linking with cross linkers (benzoquinone, chitosan, DAS, ethylene glycol-bis(succinic acid *N*-hydroxysuccinimide ester) (EG-NHS), glutaraldehyde, pectin and polyethylene glycol 8000 (PEG8000)) performed using M3 (described above) by adding the cross linkers to a final concentration of 0.01%. The CLEA suspension was left for agitation at 200 rpm for 1 h and maintained at 20 °C. Next, the CLEAs were recovered by centrifugation and washed with 0.1 M sodium phosphate buffer (pH 6) as describe above. The activity recovery of immobilized and unimmobilized CGTase G1 were calculated using the Eq. (2) and were compared.

### 2.2.8. Development of CGTase G1-CLEA using chitosan

The effect of concentration of chitosan on the properties of the final CGTaseG1-CLEA (CS-CGTG1-CLEA) was studied by varying the concentration from 0.01% to 0.20% at 20 °C for 1 h and constant shaking at 200 rpm. The effect of reaction time with chitosan was also evaluated by varying the reaction from 0.5 h to 4 h while maintaining the other parameters as described above.

## 2.3. Characterization of free and CS-CGTG1-CLEA

### 2.3.1. Optimum pH and temperature

The effect of temperature on the free and immobilized CGTase G1 was evaluated by conducting the enzyme assay at different temperatures (30 °C–90 °C) for 10 mins. The effect of pH on the enzyme activity was also investigated by conducting the enzyme assay in which the 0.1 M sodium phosphate buffer (pH 6) was replaced with buffer solutions at different pHs values ranging from pH 4–pH 10. The buffers used were 0.1 M sodium acetate buffer (pH 4 and pH 5), 0.1 M sodium phosphate buffer (pH 6, pH 7 and pH 8) and 0.1 M glycine-NaOH buffer (pH 9 and pH 10). The activity of free and immobilized CGTase G1 at different temperatures and pHs were calculated as a relative activity to the optimum condition which was defined as 100%.

### 2.3.2. Thermal stability

The thermal stability of free and immobilized CGTase G1 was determined by measuring the residual activity after 30 min incubation in absence of substrate at temperatures 50 °C, 60 °C, 70 °C and 80 °C. The samples were removed after every 5 min, chilled quickly and the residual activity was subsequently measured by phenolphthalein assay (Section 2.2.3). Activity recovery was calculated relative to the initial activity before the incubation. Initial activity at optimum condition was defined as 100%.

### 2.3.3. pH stability

The pH stability of free CGTase G1 and CGTase G1-CLEA was determined by measuring residual activity after incubation at different pHs buffer ranging from pH 4 – pH 10 for 30 min at 60 °C in the absence of substrate. The residual CGTase G1 activity was subsequently determined by phenolphthalein assay (Section 2.2.3) and activity recovery calculated relative to the initial activity before the incubation. Initial activity at optimum condition was defined as 100%.

### 2.3.4. Thermodynamic analysis

The free and immobilized CGTase G1 were incubated at 50 °C, 60 °C, 70 °C and 80 °C in absence of substrate in sodium phosphate buffer (0.1 M, pH 6). The samples were removed after 5 min intervals for a total duration of 30 min, chilled quickly and assayed for residual activity. The deactivation rate constant ( $k_d$ ) was determined when a semi-logarithmic plot of residual activity (%) was constructed at the temperatures used for inactivation versus time (min) as following:

$$\text{Slope} = k_d \quad (3)$$

Half-life ( $t_{1/2}$ ) of free CGTase G1 and CGTase G1-CLEA was calculated using Eq. (4):

$$t_{1/2} = \ln 2/k_d \quad (4)$$

Further, the Arrhenius plot where ( $\ln k_d$ ) versus ( $1/K$ ) was build and activation energy for deactivation ( $E_d$ ) was determined using Eq. (5):

$$\text{Slope} = (E_d/R) \quad (5)$$

The changes in thermodynamic parameters caused by the thermal treatment were calculated using Eyring's transition state theory [50]. The enthalpy of deactivation ( $\Delta H^\ddagger$ ) was calculated according to Eq. (6):

$$\Delta H^\ddagger = E_d - RT \quad (6)$$

where  $R = 8.314 \text{ J mol}^{-1} \text{ K}^{-1}$  is the universal gas constant and  $T =$  absolute temperature (K).

The Gibbs free energy of activation ( $\Delta G^\ddagger$ ) at different temperatures was determined using Eq. (7):

$$\Delta G^\ddagger = -RT \ln K$$

$$\Delta G^\ddagger = -RT \ln (k_d h/kT) \quad (7)$$

where  $h$  and  $k$  denote Planck's ( $6.626070 \times 10^{-34} \text{ Js}$ ) and Boltzmann's ( $1.380649 \times 10^{-23} \text{ JK}^{-1}$ ) constant, respectively.

The entropy of deactivation ( $\Delta S^\ddagger$ ) was determined using Eq. (8):

$$\Delta S^\ddagger = (\Delta H^\ddagger - \Delta G^\ddagger)/T \quad (8)$$

### 2.3.5. Kinetic study

The kinetic parameters were investigated by conducting the assay using soluble starch in a series of concentrations (1%, 2%, 3%, 4% and 5% w/v) (29 mM, 58 mM, 88 mM, 117 mM and 146 mM) in 0.1 M sodium phosphate buffer (pH 6) at 60 °C for 10 min. Reaction ( $V$ ) versus substrate concentration ( $[S]$ ) was plotted to determine the reaction order of the free and immobilized CGTase G1. Lineweaver Burk plot of  $1/V$  versus  $1/[S]$  plotted was employed for the  $V_{\max}$  and  $K_m$  calculations. The Michaelis-Menten constant ( $K_m$ ) and the maximum enzyme velocity ( $V_{\max}$ ) determined using Eq. (9) [51]:

$$\frac{1}{V_0} = \left[ \frac{K_m}{V_{\max}} \right] \cdot \left[ \frac{1}{[S]} \right] + \frac{1}{V_{\max}} \quad (9)$$

where,  $V_0$ : enzyme velocity,  $V_{\max}$ : the maximum enzyme velocity,  $K_m$ : the substrate concentration when the reaction rate is half of  $V_{\max}$ ,  $[S]$ : substrate concentration.

### 2.3.6. Fourier transform-infrared (FT-IR) analysis

The functional groups present in CLEAs were analyzed using FT-IR spectroscopy (PerkinElmer, Ohio, USA), examined in the range of 4000–400  $\text{cm}^{-1}$  in a transmittance mode. Free CGTase G1, chitosan and CS-CGTG1-CLEA were dried using an Eppendorf concentrator plus (EppendorfAG, Hamburg, Germany) and weighed samples (10 mg) were sent for analysis.

### 2.3.7. Field Emission Scanning Electron Microscopy (FESEM) analysis

The structure and morphology of immobilized CGTase G1 was examined using field emission-scanning electronic microscopy (FESEM Hitachi Ultra-high resolution SU8200 series). CLEA was dried using an Eppendorf concentrator plus (EppendorfAG, Hamburg, Germany) prior to platinum coating before FESEM analysis. Images of CLEA were taken at various magnifications.

### 2.3.8. Production of cyclodextrin (CD) and reusability analysis

The reaction of CD production was carried out for 3 h at optimum pH

and temperature (pH 6 and 60 °C) using an enzyme loading of 25 U/ g in 100 mL soluble starch (4%, w/v). Samples were withdrawn at 10, 20, 40, 60, 80, 100, 120, 140, 160 and 180 min for analysis of the  $\beta$ - and  $\gamma$ -CD concentrations using HPLC-RI. The total yield of CD production ( $Y_{CD}$ ) was calculated using Eq. (10):

$$Y_{CD} = \frac{\text{CD concentration} \left( \frac{\text{mg}}{\text{L}} \right)}{\text{Starch concentration} \left( \frac{\text{mg}}{\text{L}} \right)} \times 100 \quad (10)$$

The reusability of the CS-CGTG1-CLEA was determined for 5 cycles. After each cycle (2 h reaction), CGTase G1-CLEA were recovered by centrifugation, washed three times with 0.1 M sodium phosphate (pH 6) and then resuspended again with fresh reaction mixture. Each cycle reaction medium was then subjected to HPLC-RI to analyze the cyclodextrin synthesized. The total of CD production determined after each cycle, and the CD production of the first cycle was set as 100%.

### 2.3.9. HPLC-RI sample preparation

The concentration of  $\beta$ - and  $\gamma$ -CD were quantitated using chromatographic method described by Stregge, Huang and Risley [52] with slight modification. CDs were separated using an Xbridge™ Amide column (3.5  $\mu\text{m}$ , 4.6  $\times$  250 mm) with a flow rate of 1.0 mL/min, an injection volume of 10  $\mu\text{L}$ , where the detector temperature and column temperature were maintained at 50 °C. The mobile phase consisted of acetonitrile and water (65:35). The analysis was run for 20 min in isocratic mode. All analyses were performed using an Alliance E2695 liquid chromatography (Waters, MI, USA) equipped with a refractive index detector (RI 2424, Waters, MI, USA).

Standard were prepared by solubilizing a series of amount ranging from 1 to 12 mg/mL ( $\beta$ -CD) and 1–5 mg/mL ( $\gamma$ -CD) in acetonitrile/water (50/50) with 0.1% formic acid. The standards were filtered with a 0.2  $\mu\text{m}$  Nylon syringe filter. Each concentration was injected in triplicate and calibration curve was plotted. Samples for HPLC analysis were boiled for 10 min to stop the enzymatic reaction. The insoluble particles were filtered through a 0.2  $\mu\text{m}$  Nylon syringe filter.

### 2.4. Statistical analysis

Statistical analyses of CLEA immobilization development, screening of the cross-linkers and characterization of CGTase G1-CLEA were performed using analysis of variance (ANOVA) and Tukey's multiple-comparison post-test with GraphPad Prism 5.0 (GraphPad Software, Inc., San Diego, CA). Differences between groups of analyses were defined as not significant (represented in Figure and Table by the same letter) at a  $P$  value of  $>0.05$ . All tests were conducted in triplicate and the level of the significance was 95%.

## 3. Results and discussion

### 3.1. Homology modeling and structure refinement

Homology modeling for CGTase G1 was carried out using comparative protein modeling, with the assumption that two homologous proteins have very similar structures [53]. CGTase G1 was modelled with reasonable accuracy using a related template that was chosen based on its high percentage of sequence identity and similarity. CGTase from *Bacillus stearothermophiles* (PDB ID: 1CYG, protein resolution 2.50 Å) was chosen as the template due to its lowest E value of  $6.3 \times 10^{-227}$  and having sequence identity of 62% and similarity of 78% to CGTase G1 [36]. Homology modeling was performed using Modeller 9.13 software [54]. The 3D structure of CGTase G1 obtained was further optimized using molecular dynamic simulation by gradually minimizing its energy until it reached a stable total energy (−5965.1 kcal/mol). Verification of

the model was determined using the ERRAT and Verify3D programs as mentioned in a study done by Goh et al. (2008) and is summarized in Table S2†. The findings of this current study showed a good 3D structure based on ERRAT plot (98.03) and Verify3D program score (90.98%) with small difference in values as previously reported (98.07 and 90.99%, respectively) [36]. The model structure of CGTase G1 showed in Fig. S1†.

### 3.2. Docking analysis

In Cross-Linked Enzyme Aggregates (CLEA) formation, strong cross-linking of protein with the cross-linker is desirable to produce a stable carrier-free CLEA immobilization [20]. In this study, molecular docking techniques were used to predict the non-covalent binding of cross-linkers as ligands with CGTase G1. The 3D structure of CGTase G1 obtained from homology modeling was used as the receptor molecule, while the 3D structure of cross-linkers (benzoquinone, chitosan, dialdehyde-starch, ethylene glycol-bis(succinic acid *N*-hydroxy-succinimide ester) (EG-NHS), glutaraldehyde, pectin and polyethylene glycol 8000 (PEG8000)) obtained from the PubChem were used as the ligands. The molecular docking was performed using AutoDock Vina program. Nine different ligand binding conformations with CGTase G1 were generated. The best conformation of each cross-linker with CGTase G1 was chosen based on the lowest free energy binding ( $\Delta G$ ) which is tabulated in Table 1. The lower energy scores represent better protein-ligand binding affinity [29]. The 3D and 2D schematic diagram interaction of each cross-linker with amino acid residues of CGTase G1 is listed in Fig. S2A-G†.

Among all the cross-linkers, chitosan was found to have the lowest free energy binding with CGTase G1 (−8.0 kcal/mol) followed by EG-NHS, pectin, benzoquinone, DAS, glutaraldehyde and PEG8000 (−6.5, −6.3, −4.9, −3.7, −3.6 and −3.2 kcal/mol, respectively). Strong binding affinity is associated with a low binding energy and a low equilibrium dissociation constant value [55]. In the AutoDock Vina docking program, an empirical scoring function calculates the affinity, or fitness of protein-ligand binding by summing up the contributions of several individual terms. The binding energy is predicted as the sum of distance-dependent atom pair interaction [55]. Every atom pair has a steric interaction, which is accessed in AutoDock Vina by combining a Gaussian function with a repulsive parabolic function, which reproduces the general shape of a Lennard-Jones interaction [39].

Chitosan showed the strongest binding affinity due to the existence of the highest number of hydrogen bonds (ten hydrogen bonds) that interacted with eight residues where three of them have bond length  $< 3.00$  Å. Six residues are involved in hydrophobic interactions as seen in Fig. S2A-G†. From Table 1, chitosan showed the interaction with different types of amino acid residues (Arg, Trp, Asp, His, Tyr, Phe, His, Glu and Ala) while it was observed that the other cross-linkers interacted with fewer and same type of amino acid residues only. Based on the docking analysis, the hydrogen bond interacting with Arg365 is found to be continuously present in chitosan and EG-NHS. Ser627 interacting hydrogen bond can be found in DAS, glutaraldehyde and pectin while Thr244 hydrogen bond is present in benzoquinone and PEG8000. In addition, different hydrogen bonds were observed between different types of cross-linkers and the CGTase G1 residues, supporting the hypothesis that the nature of cross-linker chemistry correlates with the composition of enzyme surface amino acids residues.

### 3.3. Stability of docking complex system during molecular dynamic simulation

The docking results were further validated by performing MD simulation to investigate the stability of all ligand-enzyme complexes.

**Table 1**  
Computational docking analysis of cross-linkers with CGTase G1.

Cross-linker	Predicted free energy of binding ( $\Delta G$ ), kcal/mol	Hydrogen bond length ( $\text{\AA}$ )	Functional group of the ligand	Hydrogen bonds Interacting residues	Hydrophobic Interacting residues
Benzoquinone	−4.9	2.80	O1	Thr244	Met223, Gly267, Tyr237, Val3, Asp309
		2.83	O1	Thr244	
Chitosan	−8.0	3.12	O5	Arg365	Lys222, Asp219, Leu184, Tyr90, His130, His88
		3.29	O5	Arg365	
		2.94	O6	Trp91	
		3.00	O8	Asp318	
		2.85	O9	His223	
		3.24	O11	Tyr185	
		2.96	O12	Phe249	
		3.12	O13	His223	
		3.25	O13	Glu247	
		3.31	N1	Ala220	
		2.89	O1	Ser627	
Dialdehyde-starch (DAS)	−3.7	2.91	O2	Ser627	Thr230, Glu566, Met497, Leu568, Ser597, Tyr546, Ile626, Glu265, Glu598, Glu572
		2.91	O2	Ser627	
EG-NHS	−6.5	2.84	O2	Arg365	Asp186, Pro133, Tyr84, Asp361, His88, Asp318, Tyr90, Asp219, His130, Leu187, Tyr185, His80, Trp91
		2.81	O6	Tyr87	
		2.94	O6	Arg365	
		2.89	O2	Ser627	
Glutaraldehyde	−3.6	2.91	O2	Glu598	Tyr546, Glu560, Glu598, Gln572, Leu568, Thr230
		3.02	O3	Ser627	
Pectin	−6.3	2.98	O4	Glu265	Thr230, Leu568, Met497, Glu566, Ile608
		2.74	O5	Glu265	
		2.89	O5	Glu265	
		2.70	O6	Ser627	
		2.94	O6	Ser627	
		2.82	O6	Gln572	
		3.05	O1	Gly267	
		3.14	O1	Thr244	
		3.16	O1	Thr244	
		2.87	O1	Thr244	
		3.09	O1	Tyr237	
PEG8000	−3.2	2.85	O2	Tyr237	Met268, Met233, Phe243
		2.87	O2	Val242	

2-D and 3-D schematic diagram interaction of each cross-linker with amino acid residues of CGTase G1 listed in Fig. S2†.

1000 ps MD simulations for CGTase G1-crosslinker complex were performed where root mean square deviation (RMSD), root mean square of fluctuation (RMSF) and radius of gyration of complexes were computed from Gromacs utilities for further analysis. RMSD and radius of gyration values of the backbone atoms are illustrated in Fig. 1.

RMSD values were used to examine the degree of deviation for each structure and provided insight into the conformational stability of the complexes where a small deviation of structure over time indicates higher stability [56]. Based on Fig. 1A, CGTase G1 achieved its stability after 0.2 ns where the fluctuation was between 0.2 nm to 0.3 nm, whereas for CGTase G1 with cross-linker complex, all complexes showed lower RMSD values than CGTase G1, indicating that the presence of cross-linkers increases their stability over time. The most stable complex was CGTase G1 with pectin, with a degree of deviation of only 0.13 nm to 0.15 nm, followed by PEG8000, EG-NHS and benzoquinone (deviation was between 0.15 nm to 0.2 nm). While CGTase G1 with glutaraldehyde showed the same RMSD values until 0.6 ns before equilibrating at smaller RMSD values. On the other hand, RMSD values for CGTase G1 with DAS and chitosan increase over time and showed higher deviation (both between 0.15 nm to 0.25 nm) respectively.

Compactness and rigidity of CLEA structure were also factors in its improved performance [20,57]. Hence, radius of gyration of CGTase G1-crosslinker complex was investigated and the results are presented in Fig. 1B. The smaller size of CLEA not only causes mass loading issues in real-industrial applications, but its high compactness and rigidity also contributed to low immobilized activity recovery due to substrate diffusion limitations [21]. Based on Fig. 1B, the presence of cross-linkers decreased the size of radius in CGTase G1 complex. Among all the cross-linkers, CGTase G1 with EG-NHS showed the smallest radius (2.51 nm) followed by pectin (2.53 nm). CGTase G1 with benzoquinone,

glutaraldehyde and PEG8000 showed the same average radius of gyration (2.55 nm), while CGTase G1 with chitosan and DAS recorded the highest radius of gyration (2.56 nm) compared to CGTase G1 only (2.58 nm). The larger size of CGTase G1 with chitosan and DAS complexes is more beneficial in the CLEA development as it can tackle the mass loading problem in real industrial applications [20].

Root mean square fluctuations (RMSF) of the backbone atom of each residue in the CGTase G1 and complexes was analyzed to observe the flexibility of the enzyme backbone structure. High RMSF value indicates higher flexibility whereas low RMSF shows the rigidity of the complex [56]. The RMSF of CGTase G1 was compared with CGTase G1-crosslinker complexes as shown in Fig. 2. Strong cross-linking improves the performance of the immobilized enzyme in the CLEA formation, as previously stated. However, cross-linking at the active site region in this case especially at the CGTase G1 catalytic triad (Asp 251, Glu 279 and Asp 350) that is responsible for converting the substrate into product may inhibit the activity recovery of CLEA. The CGTase G1-chitosan complex showed the highest RMSF values at active site region, followed by DAS, benzoquinone, EG-NHS, glutaraldehyde, pectin and finally PEG8000. CGTase G1-chitosan complex that displayed higher fluctuation numbers at the catalytic triad where high flexibility in the active site may contribute to high activity of CGTase G1-CLEA compared to others.

From our computational data, macromolecule cross-linkers (chitosan followed by DAS) were predicted to be the best cross-linker for CGTase G1. Chitosan and DAS are linear- structured polymers that allows the bonding of enzyme molecules along its long chain. Macromolecule chitosan or DAS will form a less clumped CLEA particle, thus promoting higher accessibility to active site hence increasing the enzymatic activity [58,59]. While, glutaraldehyde and the other cross-linkers such as

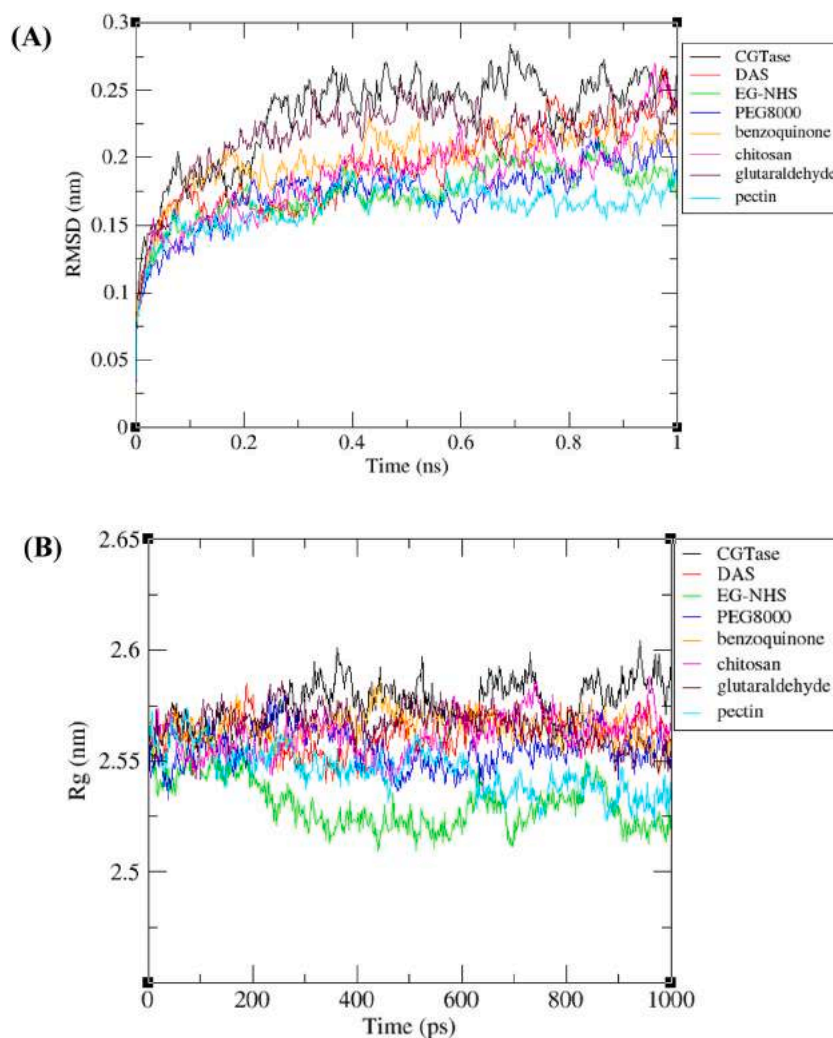


Fig. 1. (A) Root mean square deviation values and (B) Radius of gyration analysis of CGTase G1 and CGTase G1-crosslinker complexes.

benzoquinone, EG-NHS, pectin and PEG8000 are smaller molecules compared to chitosan and DAS that can penetrate the inner part of the enzyme and interact with amino acid residues that are vital for enzymatic activity [28] which could also cause formation of compact structure of CGTase G1-CLEA. Experiments were thus conducted to confirm these results.

### 3.4. Development of CGTase G1-CLEA

Generally, the preparation of CLEA involves an aggregation step by adding a precipitant, followed by the cross-linking process with the cross linker [20]. CLEA stability and catalytic activity are markedly affected by several factors such as type of precipitating agents, type of cross linkers, cross-linkers concentration, cross-linking time, temperature, and agitation. Therefore, these parameters were optimized to develop the CLEA with the highest activity recovery [22].

Precipitants and precipitation condition play a crucial role in the preparation of CLEAs. They can induce a more active conformation of the enzyme, in such a way that selectivity of CLEAs strongly depends on the conformation of the aggregates [20]. Several water miscible organic solvents (ethanol, acetonitrile, methanol, isopropanol, tert-butanol, dimethylformamide (DMF), acetone and dimethyl sulfoxide (DMSO)) were screened as the precipitating agents for CGTase G1. The precipitated CLEAs were recovered by centrifugation and re-dispersed in 0.1 M sodium phosphate buffer (pH 6). Fig. 3A shows that among the precipitants evaluated, tert-butanol yielded the highest precipitation yield

recovery ( $95.6 \pm 1.21\%$ ) while methanol gave the lowest yield of  $3.8 \pm 0.82\%$ . This finding is similar to Abdul Wahab et al. [60] where tert-butanol was found to be the best precipitant that resulted in the highest xylanase-CLEA activity recovery.

The effect of tert-butanol concentration and precipitation time were also evaluated. Different volumetric concentrations of tert-butanol from 70% to 90% (v/v) were utilized and the result are shown in Fig. S3†. Similar results were yielded when 75% to 90% tert-butanol was used ( $95.8 \pm 0.51\%$ ). Time of precipitation was recorded from 15 min to 75 min and the results (Fig. S4†) showed that the maximum precipitation activity ( $95.1 \pm 0.64\%$ ) was reached at 1 h time. Consequently, 75% of tert-butanol at 1 h precipitation was selected for aggregation in CGTase G1-CLEA preparation.

To screen and compare the different cross-linkers towards CGTase G1-CLEA, glutaraldehyde was selected as a model cross-linker and parameters namely glutaraldehyde concentration and time of cross-linking were optimized. Glutaraldehyde is the cross-linking agent most frequently used as it is water soluble and commercially available [23]. The ratio of cross-linker to enzyme is an important factor; if the ratio is too low, not enough cross-linking occurs, and CLEA does not form properly. However, excess cross-linker can result in a complete loss of enzyme flexibility thus affecting the activity recovery [20,61].

Fig. 3B shows the activity recovery of CGTase G1-CLEA using 0.005% to 0.2% glutaraldehyde (v/v at final concentration) and activity in the supernatant for the first washing solution indicates the activity lost in relation to the total CGTase initial activity. Cross-linking with

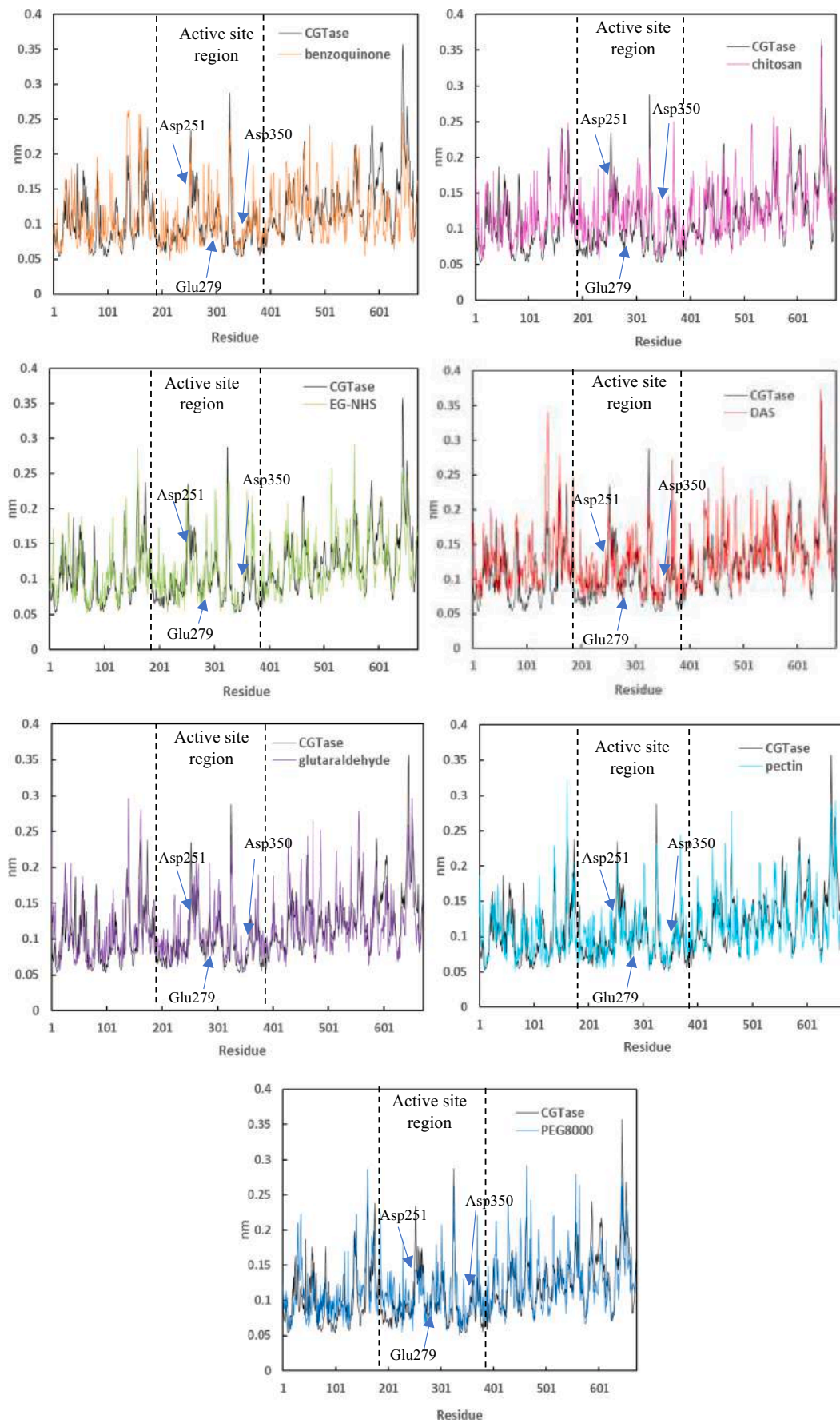
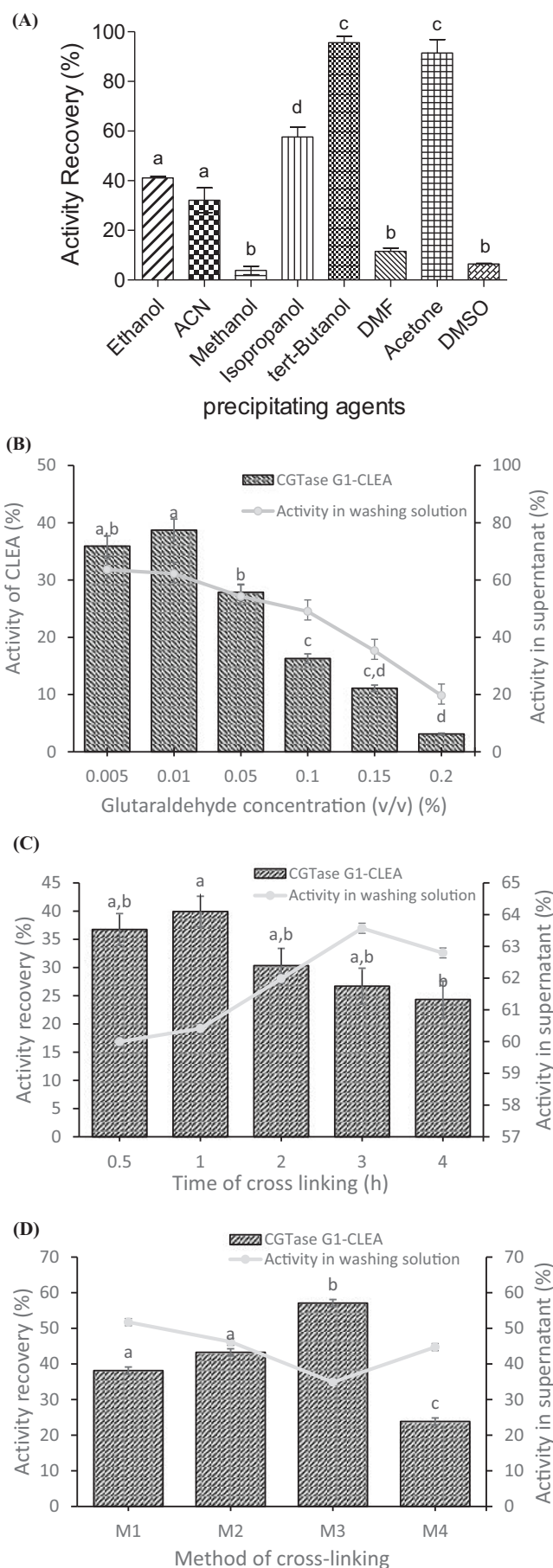


Fig. 2. Root mean square fluctuation values of CGTase G1 and CGTase G1-crosslinker complexes.



**Fig. 3.** (A) Precipitation of CGTase G1 with different precipitation agents (B) Cross-linking of CGTase G1 with different concentration of glutaraldehyde for 1 h, 20 °C at 200 rpm agitation after precipitation with 75% tert-butanol. (C) Effect of cross-linking time with 0.01% glutaraldehyde (D) Different method in preparation of CGTase G1-CLEA using 0.01% glutaraldehyde. The total initial CGTase activity (100 ± 10 U/mL) was set as 100%. The experiments were performed in triplicate and the error bar represent the standard deviation error in each of readings. Mean values with the significant differences appear by distinct letters when  $P < 0.05$  by the ANOVA Tukey test.

0.01% glutaraldehyde permitted the highest CLEA activity recovery ( $38.7 \pm 1.5\%$ ) while  $62.2 \pm 1.0\%$  activity loss was observed in the first washing solution. Moreover, it was found that higher concentrations of glutaraldehyde allowed for cross-linking since activity lost in the supernatant decreased from 40% to 15%. However, the activity of CLEA recovered also dropped at higher concentrations. This low activity recovery could be associated with diffusional problems of the large substrate within the supramolecular structure of CLEA or inactivation induced by glutaraldehyde because the extensive cross-linking may cause a distortion of the enzyme structure [23].

Next, cross-linking time was evaluated using 0.01% glutaraldehyde and the results are presented in Fig. 3C. The activity of recovered CLEA yielded the highest activity at one-hour cross-linking before decreasing over time. Increasing activity in washing solution over time was observed, consequently affecting the CLEA activity recovery (Fig. 3C). This may be due to the reversible interactions between glutaraldehyde and CGTase over time [62].

Slight modification to the common method in CLEA preparation were carried out. Method 1 (M1) developed by Cao et al. [63] and subsequently marketed by CLEA Technologies (Holland) has been used widely in CLEA development involving precipitation, followed by the addition of the cross-linker sequentially [22]. The common method has a limitation in that there is a potential interaction between the cross-linker and the precipitating agents, which could affect the cross-linker reactive functional group, inhibiting the cross-linking process and adversely affecting CLEA's overall activity. Hence, in this study Method 2 (M2), 3 (M3) and 4 (M4) were developed to investigate this effect and the results are illustrated in Fig. 3D.

As shown in Fig. 3D, it was discovered that the activity of CLEA recovery increased when segregating the precipitating reagent with the cross-linker in cross-linking process. CLEA developed using M2 yielded  $43.3 \pm 0.04\%$  while using M3 yielded  $53.1 \pm 0.05\%$  activity recovery compared to when using the common M1 ( $38.1 \pm 0.03\%$ ). While simplified Method 4 (M4) that combines the precipitation and cross-linking simultaneously was observed to produce the lowest activity recovery ( $23.8 \pm 0.05\%$ ). Based on activity in the first washing solution, CLEA developed with M3 showed the least enzyme loss ( $34.9 \pm 0.02\%$ ), followed by M2 and M4 ( $44.7 \pm 0.08\%$  and  $46.2 \pm 0.05\%$ , respectively), with M1 showing the most enzyme loss ( $51.7 \pm 0.03\%$ ). Based on this data, adding glutaraldehyde after tert-butanol precipitation has an effect on CLEA formation. Unspecific interaction of glutaraldehyde with tert-butanol might alter the active functional group, resulting in weak or reversible interaction of glutaraldehyde with CGTase G1 in CLEA. CLEAs developed with M3 yielded higher activity recovery compared to M2 which in this case, centrifugation of precipitate before cross-linking in M2 may increase the compactness of the structure leading to substrate diffusion limitation. Therefore, M3 was selected as the method to prepare the CGTase G1-CLEA throughout this study.

### 3.5. Screening of different type of cross-linkers and development of CS-CGTG1-CLEA

Consequently, using the above optimized method (M3), CGTase G1-CLEAs were developed using several different cross-linkers (benzoquinone, chitosan, DAS, EG-NHS, pectin and PEG8000) and the results are illustrated in Fig. 4A. CGTase G1-CLEAs using cross linkers with the

(caption on next column)

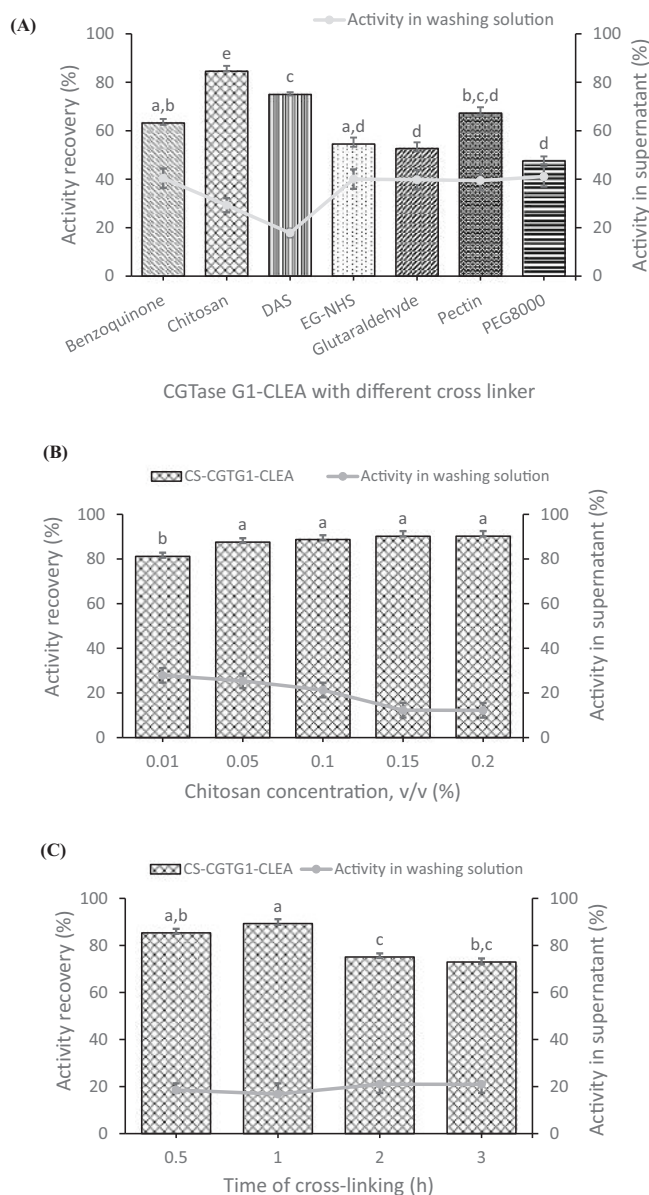


**Fig. 4.** (A) Screening of different type of cross-linkers in developing of CGTase G1-CLEA. Cross-linking was maintained for 1 h, 20 °C at 200 rpm agitation with fixed cross-linkers concentration (0.01%) (B) Cross-linking of CGTase G1 with different concentration of chitosan (C) Effect of cross-linking time with 0.15% chitosan. CLEA were recovered by centrifugation and washed with buffer three times for activity recovery determination. First washed solution was taken to evaluate the activity loss. The total initial CGTase activity (100 ± 10 U/mL) was set as 100%. The experiments were performed in triplicate. Mean values with the significant differences appear by distinct letters when  $P < 0.05$  by the ANOVA Tukey test.

highest activity recovery to the lowest activity recovery related to free CGTase G1 activity are as follows: chitosan (84.6 ± 0.26%) > DAS (74.9 ± 0.39%) > pectin (67.3 ± 0.67%) > benzoquinone (63.2 ± 0.81%) > EG-NHS (54.5 ± 1.11%) > glutaraldehyde (52.7 ± 1.18%) > PEG8000 (47.6 ± 1.36%). Meanwhile, CGTase G1-CLEAs developed using DAS showed the least enzyme loss (17.8 ± 1.74%) based on the activity in washing solution followed by chitosan (29.3 ± 1.01%), whereas the others showed about the same amount of activity loss which was 40%.

Previously, Rojas et al. [24] developed CLEA of a thermostable CGTase from *Thermoanaerobacter* sp. using glutaraldehyde and macromolecular agents (starch-aldehyde and pectin-aldehyde) as the cross-

linkers. Starch-aldehyde produced the most active CLEA (24% activity recovery) compared to glutaraldehyde which only maintained around 10% of its initial activity. On the other hand, Zhang et al. [25] reported that CLEA of CGTase from *Komagataellaphaffii* sp. maintained 4.6% activity recovery when cross-linked with glutaraldehyde. In this study, a modified method was used to prepare the CLEA, and it was found that glutaraldehyde and DAS were able to produce higher CGTase G1-CLEA activity than in previous studies [24,25], and that using other cross-linkers like chitosan permitted even higher activity recovery.

This result was also supported by earlier docking analysis and molecular dynamic simulations of the CGTase G1-crosslinker complex, which predicted chitosan as the best cross-linker for CGTase G1. High binding affinity, flexibility based on RMSF values, and low compactness based on radius of gyration analysis from computational data shown by CGTase G1 with chitosan complex could be contributing factors for the highest CGTase-CLEA activity recovery obtained experimentally as shown in Fig. 4A. In CLEA immobilization, chitosan was first reported as a cross-linking agent by Arsenault et al. [58] in the development of Laccase-CLEA. Later, this renewable biopolymer chitosan became an attractive candidate for the cross-linking of the enzyme aggregates because of its high amino group content which favors link formation with enzymes. Moreover, chitosan showed good mechanical strength, high resistance to chemical degradation, in addition to its biocompatibility and biodegradability [64].

To validate the docking analysis with the experimental data, CGTase G1-CLEA cross-linked with chitosan (CS-CGTG1-CLEA) was further optimized and characterized. Parameters namely chitosan concentration and time of cross-linking were optimized to obtain the highest CS-CGTG1-CLEA activity recovery and the results are illustrated in Fig. 4B and Fig. 4C. The highest CS-CGTG1-CLEA activity was obtained (90.2 ± 0.45%) when the chitosan concentration was 0.15% (v/v) (Fig. 4B) and crosslinked for 1 h (Fig. 4C). This significantly improved the CS-CGTG1-CLEA activity recovered by 6% over the earlier screening phase using 0.01% chitosan concentration (84.6 ± 0.26%) (Fig. 4A).

Fig. 4B shows that the enzyme lost in the washing solution decreases as the chitosan concentration increases indicating increasing immobilization efficiency. However, as the cross-linking time increases, CS-CGTG1-CLEA activity recovery declined (Fig. 4C). This may have occurred as a result of extensive cross-linking, which altered the enzyme conformation, resulting in substrate diffusional limitation [20]. However, based on molecular dynamic simulation data analysis in Fig. 2, CGTase G1-chitosan complex showed high variation compared to other cross-linkers based on RMSD analysis, indicating that the interaction was unstable over time. Thus, it was predicted an increase in washing solution at higher time of cross-linking can be attributed to unstable interaction of chitosan over time.

### 3.6. Characterization of free CGTase G1 and CS-CGTG1-CLEA

#### 3.6.1. Influence of temperature and pH

Influence of temperature on the relative activities of free and immobilized CGTase G1 was monitored by measuring CGTase G1 activity as a function of temperature in the range of 40 °C to 80 °C. CS-CGTG1-CLEA was observed to have the same optimum temperature with native CGTase G1 which is at 60 °C (Fig. 5A). CLEA remarkably preserved greater activities at higher temperature compared to free enzyme, while the effect of pH on the activity profiles of free and CS-CGTG1-CLEA was assessed in the range of pH 4–pH 10 and the results are shown in Fig. 5B. Optimum pH value for both free and immobilized CGTase G1 was shown to be pH 6. Immobilized CGTase G1-CLEA displayed higher relative activity at both acidic and alkaline pH conditions except at pH 7 compared to free enzyme.

Consequently, thermal stability assessment of free and CS-CGTG1-CLEA were performed by incubating both enzymes in absence of substrate at different temperatures 50 °C–80 °C for 30 min before the standard assay was conducted to determine the activity recovery. The

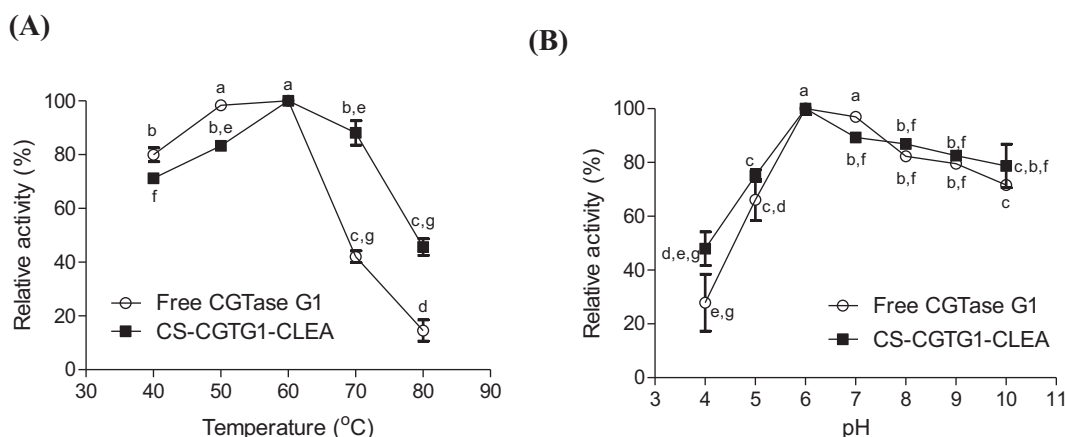


**Fig. 5.** (A) Optimum temperature (B) Optimum pH of free CGTase G1 and CS-CGTG1-CLEA. Enzyme activity of free and CS-CGTG1-CLEA at optimum temperature and pH was defined as 100%. The experiments were performed in triplicate and the error bar represent the standard deviation error in each of readings. Mean values with the significant differences appear by distinct letters when  $P < 0.05$  by the ANOVA Tukey test.

results are highlighted in Fig. 6A–D. After 30 min incubation, CLEA showed higher thermal stability than free enzyme at all temperatures tested (Fig. 6A–D). After immobilization, the conformational flexibility or rigidity of the enzyme decreased, hence increasing the thermal resistance of the enzyme. As a result, the enzyme requires higher activation energy to attain proper functional conformation [65]. From Fig. 6A, both CS-CGTG1-CLEA ( $88.24 \pm 1.13\%$ ) and free enzyme ( $74.19 \pm 1.09\%$ ) were observed to preserve a good activity recovery after 30 min incubation at temperature  $50\text{ }^{\circ}\text{C}$ . However, a distinct difference between free and immobilized CGTase G1-CLEA were observed when both were incubated at higher temperatures of  $60\text{ }^{\circ}\text{C}$ ,  $70\text{ }^{\circ}\text{C}$  and  $80\text{ }^{\circ}\text{C}$ . At temperature  $60\text{ }^{\circ}\text{C}$  (Fig. 6B), free enzyme activity recovery started to decline tremendously from its initial activity after 20 min incubation ( $13.31 \pm 1.01\%$ ) before dropping to  $5.51 \pm 2.10\%$  after 30 min incubation while CS-CGTG1-CLEA maintained  $83.07 \pm 1.21\%$  (after 20 min) and  $52.73 \pm 0.93\%$  of its activity recovery after 30 min incubation. At higher temperature of  $70\text{ }^{\circ}\text{C}$  (Fig. 6C), CS-CGTG1-CLEA maintained  $32.26 \pm 0.83\%$  activity whereas free CGTase G1 retained only  $4.47 \pm 0.87\%$  of their relative activities after 30 min incubation. Furthermore, CGTase G1-CLEA presented  $21.72 \pm 2.03\%$  of its relative activity after 30 min at  $80\text{ }^{\circ}\text{C}$  (Fig. 6D) while the free enzyme was found to be nearly inactive as early as 5 min incubation which retained  $0.01 \pm 1.19\%$  relative activity at the same temperature. From this result, it was suggested that the thermal stability of CGTase G1 was enhanced after the CLEA was formed and was not prone to rapid degradation and inactivation at various temperatures and susceptible at long-term storage.

pH stability of free and CS-CGTG1-CLEA were conducted by incubating both enzymes in buffer with different pHs (Fig. 6E) at  $60\text{ }^{\circ}\text{C}$  for 30 min without substrate followed by standard assay to determine the activity recovered. Based on Fig. 6E, immobilized CGTase G1 showed stability in both acidic and alkaline conditions, while free enzyme only can maintain about 2%–6% of its relative activity after incubation in buffers at pH 4–10 for 30 min. CS-CGTG1-CLEA preserved a greater activity at pH 6 ( $50.19 \pm 2.11\%$ ) and pH 7 ( $32.75 \pm 2.09\%$ ) (Fig. 6E). These results were in agreement with a study by Nawawi et al. [28] which also used chitosan as the cross-linker for Mag1-CLEA that found a greater stability at pH 6 and pH 7. The stability of CGTase G1-CLEA in the alkaline buffer (pH 8, 9 and 10) suggested that cross linking of amino group of enzyme/chitosan promotes acidic environment for the enzyme, thus, the addition of alkaline pHs buffer can neutralize acidic groups and is favorable to stabilize the enzyme [28]. The cross-linking process in CLEA stabilizes the enzyme structure and protects enzyme subunit dissociation [66], thus preserving CGTase G1-CLEA activity recovery at various range of pHs.

### 3.6.2. Thermal deactivation and thermodynamic analysis

The prospect of the immobilized enzyme to withstand high temperature is a major advantage in terms of industrial enzyme application [67]. Thermal deactivation was examined by incubating the free CGTase G1 and CS-CGTG1-CLEA without substrate at different temperatures ( $50\text{ }^{\circ}\text{C}$ ,  $60\text{ }^{\circ}\text{C}$ ,  $70\text{ }^{\circ}\text{C}$  and  $80\text{ }^{\circ}\text{C}$ ) for different time intervals (every 5 min for 30 min) and determined based on the thermal deactivation constant ( $k_d$ ) obtained from the gradient of the pseudo-first plot illustrated at Fig. S5†. Half-life ( $t_{1/2}$ ) which is the time required to reduce 50% of the initial enzyme activity at a particular temperature was also determined from the same plot.

The values of respective  $k_d$  and their  $t_{1/2}$  at different temperatures are summarized in Table 2. Overall, the value of  $k_d$  increased while their  $t_{1/2}$  decreased at higher incubated temperature for both free and immobilized CGTase G1. The thermal deactivation constants observed for CS-CGTG1-CLEA were  $0.42 \pm 0.1\text{ min}^{-1}$ ,  $0.73 \pm 0.2\text{ min}^{-1}$ ,  $0.47 \pm 0.1\text{ min}^{-1}$ ,  $0.65 \pm 0.2\text{ min}^{-1}$  fold smaller than free enzyme, whereas half-life of CS-CGTG1-CLEA showed 0.71, 1.92, 1.41, and 1.84 min fold longer than free enzyme at temperatures of  $50\text{ }^{\circ}\text{C}$ ,  $60\text{ }^{\circ}\text{C}$ ,  $70\text{ }^{\circ}\text{C}$  and  $80\text{ }^{\circ}\text{C}$ , respectively.

From the  $k_d$  values obtained, the thermodynamic and kinetic parameters, enthalpy ( $\Delta H^{\#}$ ), Gibbs free energy ( $\Delta G^{\#}$ ) and entropy ( $\Delta S^{\#}$ ) of deactivation were calculated using the equation from the Arrhenius plot (Fig. S5†) and presented in Table 2. Thermodynamic data represents another method for assessing enzyme stability and interpreting its catalytic and physiological properties [68]. Enthalpy of deactivation ( $\Delta H^{\#}$ ) generally measures the number of noncovalent bonds that are broken hence representing the total amount of energy required during enzyme denaturation. However,  $\Delta H^{\#}$  values obtained are not temperature-dependent parameters and these values alone are unsuitable indicators for determining the enzyme stability [65]. As shown in Table 2, on average,  $\Delta H^{\#}$  values of free enzyme is higher ( $72.95 \pm 0.11\text{ kJ/mol}$ ) than immobilized CS-CGTG1-CLEA ( $66.83 \pm 0.11\text{ kJ/mol}$ ). No change in enzyme heat capacity for free and CS-CGTG1-CLEA was observed at their specific range of temperatures (Table 2). Both free and immobilized CGTase G1 portrayed positive  $\Delta H^{\#}$  values indicating the endothermic nature of denaturation reaction.  $\Delta H^{\#}$  values decreased after CLEA was formed with reference to free enzyme and remained constant at all temperatures tested. This is in agreement with a study done by Rehman et al. [68] and Abd Rahman et al. [65].

Thus, the determination of Gibbs free energy ( $\Delta G^{\#}$ ) of the inactivation process is more accurate and reliable for predicting and evaluating enzymes stability.  $\Delta G^{\#}$  is the energy barrier for enzyme deactivation which can determine the enzyme thermostability besides the spontaneity of deactivation processes of thermal unfolding [69]. From Table 2,

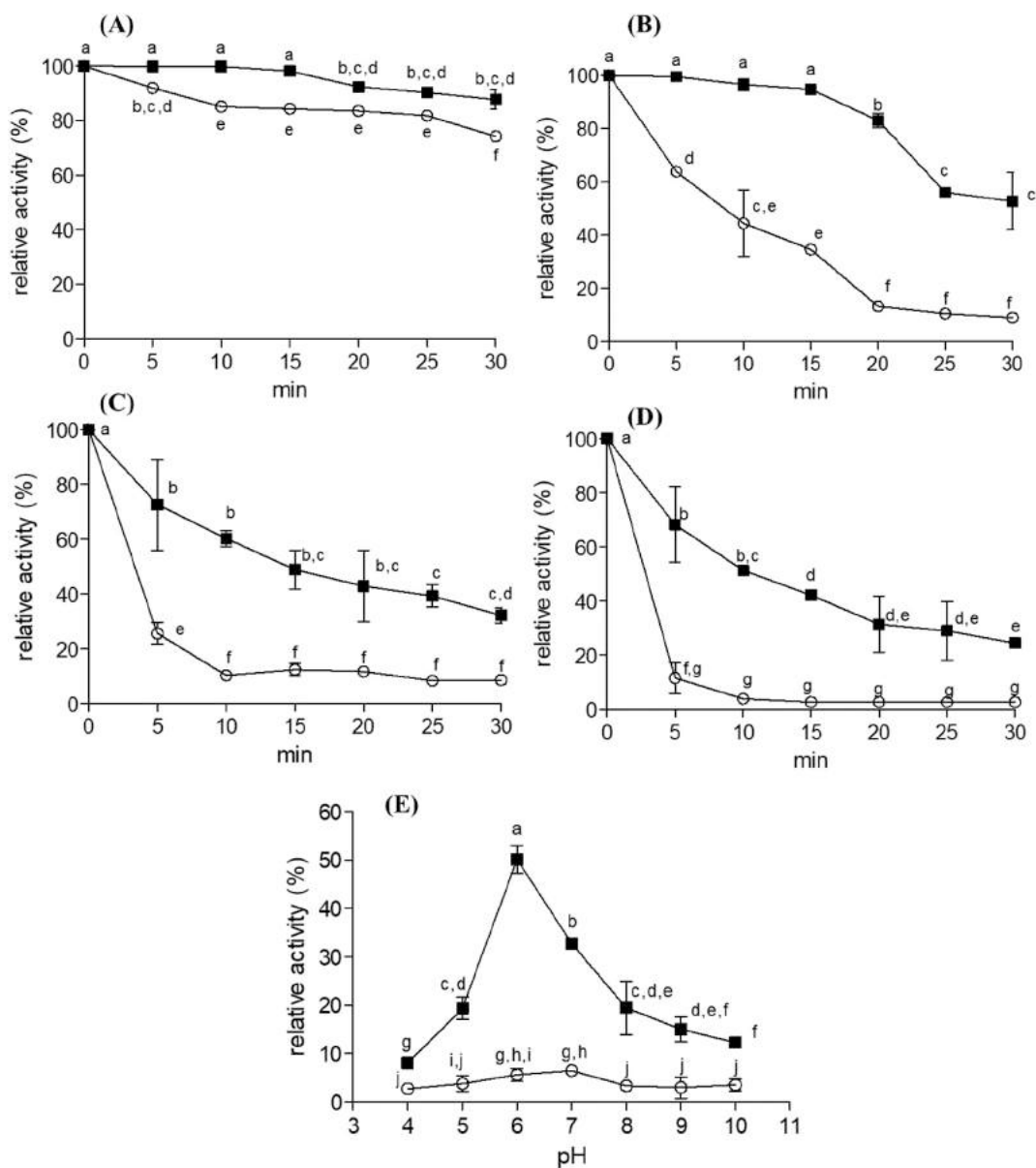


**Fig. 6.** Thermal stability of free CGTase G1 (○) and CS-CGTG1-CLEA (■) at temperature (A) 50 °C (B) 60 °C (C) 70 °C (D) 80 °C. (E) pH stability of free CGTase G1 (○) and CS-CGTG1-CLEA (■). Initial CGTase G1 and CS-CGTG1-CLEA activity was set as 100%. The experiments were performed in triplicate and the error bar represent the standard deviation error in each of readings. Mean values with the significant differences appear by distinct letters when  $P < 0.05$  by the ANOVA Tukey test.

**Table 2**

Thermal deactivation kinetic and thermodynamic parameters of free CGTase G1 and CS-CGTG1-CLEA.

	50 °C		60 °C		70 °C		80 °C	
	Free enzyme	CLEA	Free enzyme	CLEA	Free enzyme	CLEA	Free enzyme	CLEA
$k_d$ (min <sup>-1</sup> )	0.0082 ± 0.00 <sup>u</sup>	0.0048 ± 0.00 <sup>v</sup>	0.0673 ± 0.01 <sup>p,q</sup>	0.0231 ± 0.02 <sup>t</sup>	0.0860 ± 0.01 <sup>o,p</sup>	0.0357 ± 0.01 <sup>r</sup>	0.133 ± 0.07 <sup>o</sup>	0.0469 ± 0.03 <sup>s,t</sup>
$t_{1/2}$ (min)	84.61 ± 2.12 <sup>b</sup>	144.71 ± 2.92 <sup>a</sup>	10.30 ± 1.34 <sup>l</sup>	30.06 ± 3.05 <sup>s,h</sup>	8.06 ± 1.51 <sup>h,m</sup>	19.41 ± 1.73 <sup>i,j</sup>	5.21 ± 1.94 <sup>n</sup>	14.80 ± 1.23 <sup>k</sup>
$\Delta H^\#$ (kJ/mol)	73.08 ± 3.13 <sup>c</sup>	67.08 ± 2.14 <sup>c,d</sup>	73.00 ± 3.02 <sup>c</sup>	67.00 ± 2.24 <sup>c,d</sup>	72.91 ± 2.95 <sup>c</sup>	66.92 ± 2.99 <sup>c,d</sup>	72.83 ± 2.99 <sup>c</sup>	66.83 ± 3.01 <sup>c,d</sup>
$\Delta G^\#$ (kJ/mol)	61.22 ± 2.38 <sup>d,e</sup>	62.66 ± 2.01 <sup>d,e</sup>	56.52 ± 3.12 <sup>e</sup>	60.16 ± 1.93 <sup>e</sup>	58.83 ± 3.11 <sup>e</sup>	60.64 ± 2.21 <sup>d,e</sup>	58.46 ± 3.09 <sup>e</sup>	61.52 ± 1.09 <sup>d,e</sup>
$\Delta S^\#$ Jmol <sup>-1</sup> K <sup>-1</sup>	36.70 ± 2.02 <sup>g</sup>	13.69 ± 1.99 <sup>k</sup>	50.99 ± 2.54 <sup>e,f</sup>	21.16 ± 1.32 <sup>i,j</sup>	43.58 ± 1.11 <sup>f</sup>	19.44 ± 2.18 <sup>i,j</sup>	44.47 ± 3.09 <sup>f</sup>	16.44 ± 3.01 <sup>i,j</sup>

$k_d$  = thermal deactivation rate constant,  $t_{1/2}$  = half-life,  $\Delta H^\#$  = change in enthalpy,  $\Delta G^\#$  = change in Gibbs free energy and  $\Delta S^\#$  = change in entropy of deactivation. Mean values with the significant differences appear by distinct letters when  $P < 0.05$  by the ANOVA Tukey test.

$\Delta G^\#$  values of CS-CGTG1-CLEA were larger than free enzyme at all tested temperatures. CS-CGTG1-CLEA showed higher  $\Delta G^\#$  values by 2.4%, 2.3%, 7.3% and 5.2% compared to free enzyme at temperatures of 50 °C, 60 °C, 70 °C and 80 °C, respectively. Positive values of  $\Delta G^\#$  for both free and immobilized CGTaseG1-CLEA indicated that the thermal

deactivation process is thermodynamically non-spontaneous [70] and larger value of  $\Delta G^\#$  for CS-CGTG1-CLEA compared to free CGTase G1 stipulates its high resistance to the denaturation.

The entropy ( $\Delta S^\#$ ) measures the degree of variation or orderliness between the ground state and transition state of enzymes molecules

**Table 3**Kinetic analysis of free and immobilized CGTase G1 on cyclization of  $\beta$ -CD.

Kinetic parameters	$K_m$ (mM)	$V_{max}$ (mM.min <sup>-1</sup> )	$k_{cat}$ (s <sup>-1</sup> )	Catalytic efficiency ( $k_{cat}/K_m$ ) (mM <sup>-1</sup> s <sup>-1</sup> )
Free CGTase G1	8.93 $\pm$ 0.74 <sup>c</sup>	9.80 $\pm$ 0.01 <sup>c</sup>	402.89 $\pm$ 1.21 <sup>a</sup>	45.12 $\pm$ 1.11 <sup>b</sup>
CS-CGTG1-CLEA	9.87 $\pm$ 0.25 <sup>c</sup>	9.87 $\pm$ 0.03 <sup>c</sup>	405.77 $\pm$ 2.19 <sup>a</sup>	41.11 $\pm$ 2.15 <sup>b</sup>

Mean values with the significant differences appear by distinct letters when  $P < 0.05$  by the ANOVA Tukey test.

[68]. From Table 2, both  $\Delta S^\ddagger$  values of free and immobilized CGTase G1-CLEA increased from temperature 50 °C to 60 °C before decreasing at higher temperature tested. Overall,  $\Delta S^\ddagger$  values of CS-CGTG1-CLEA were 0.63, 0.58, 0.55, 0.60 Jmol<sup>-1</sup> K<sup>-1</sup> fold smaller than free enzyme generally because immobilization imparts rigidity, consequently increasing its order. Immobilization of CGTase from *Bacillus amyloliquifaciens* onto different carriers by Abdel-Naby et al. [71] supports the thermal deactivation and thermodynamic results of this study. When compared to free CGTase, immobilized CGTase had a lower activation energy, a lower deactivation constant rate, a longer half-life, and decreased  $\Delta S^\ddagger$  and  $\Delta H^\ddagger$  values [71].

### 3.6.3. Kinetic performances of free immobilized CGTase G1-CLEA

Enzyme kinetic was analyzed to determine the reaction rate of free and immobilized CGTase G1-CLEA at different substrate concentrations. It was shown that when the production of  $\beta$ -CD against 1% (29 mM), 2% (58 mM), 3% (88 mM), 4% (117 mM) and 5% (w/v) (146 mM) starch concentration was plotted, free and CS-CGTG1-CLEA obeyed the Michaelis-Menten plot (Fig. S6†). Maximal velocity ( $V_{max}$ ), turn over number ( $k_{cat}$ ) and Michaelis-Menten constant ( $K_m$ ) were determined by plotting a Linearweaver-Bluk plot (Fig. S7†) and the results are tabulated in Table 3.

From Table 3, at the same concentration of enzymes used, both free and CS-CGTG1-CLEA displayed the same  $V_{max}$  and  $k_{cat}$  values (9.80  $\pm$  0.10 mM/min and 404.33  $\pm$  0.2 s<sup>-1</sup>). However,  $K_m$  of free enzyme (8.93  $\pm$  0.24 mM) was slightly smaller than CS-CGTG1-CLEA (9.87  $\pm$  0.25 mM). The smaller  $K_m$  value of the free enzyme indicates higher substrate binding, hence demonstrating its increased efficiency of substrate conversion compared to CS-CGTG1-CLEA. Immobilization of CGTase on different supports such as chitin, Amberlite IRA-45, Duolite and polyacrylamide were also displayed higher  $K_m$  than free enzyme [71]. This increase of the  $K_m$  value after immobilization may be partially due to mass transfer resistance of the substrate into the active site of immobilized enzyme. From Table 3, CS-CGTG1-CLEA appeared to be less specific (41.11  $\pm$  0.15 mM<sup>-1</sup> s<sup>-1</sup>) than free enzyme (45.12  $\pm$  0.11 mM<sup>-1</sup> s<sup>-1</sup>). However, small differences in kinetic properties for both free CGTase G1 and CS-CGTG1-CLEA might be influenced by the activity recovery of CS-CGTG1-CLEA (90.2  $\pm$  0.45%) compared to free enzyme.

$K_m$  value is associated with substrate binding of the enzyme where the smaller the  $K_m$  value (substrate concentration reached 50% of the  $V_{max}$ ), the better the binding of the substrate hence increasing its efficiency of substrate conversion in the active site. In the free form of CGTase, the catalytic site is able to convert the substrate into product without any interference. Hence, from these results, it can be deduced that cross-linking of CGTase G1 with chitosan does not adversely affect the catalytic performance of CS-CGTG1-CLEA. This result indirectly supports the radius of gyration (Fig. 1B) and RMSF (Fig. 2) data analysis from the CGTase G1-chitosan complex molecular dynamic simulation done earlier. CGTase G1-chitosan complex showed the highest fluctuation based on RMSF at active site region of CGTase G1 indicating its flexibility and large radius of gyration which may have discarded the substrate diffusion limitation. Catalytic performance and substrate diffusion limitation are common drawbacks in the development of CLEAs [20,57], but this was not the case with CS-CGTG1-CLEA, which appeared to have the same catalytic performance as free enzyme.

### 3.6.4. FT-IR analysis of CS-CGTG1-CLEA

Interaction of free CGTase G1 with chitosan in CLEA immobilization

was analyzed based on the functional group present in the FT-IR spectra (Fig. S8†). Based on FT-IR spectrum of free CGTase G1, the peaks indicating that zwitterions compound of amino acids which exhibit the combinations of carboxylate (COO<sup>-</sup>) and primary amine salts (NH<sub>3</sub><sup>+</sup>) was observed. Amino acids in free enzyme showed that NH<sub>3</sub><sup>+</sup> stretch is absorbed at 2792 cm<sup>-1</sup> (broad) and N—H bend at 1645 cm<sup>-1</sup>, while symmetry COO<sup>-</sup> stretch peak appeared at 1280 cm<sup>-1</sup>. When compared with FT-IR spectrum of chitosan alone, new peaks appeared at CS-CGTG1-CLEA, absorbed at wavenumbers 2235 cm<sup>-1</sup> and 2177 cm<sup>-1</sup> and these peaks also appeared at free enzyme spectrum which confirmed the presence of CGTase G1 in CLEA. Meanwhile, from the molecular docking analysis (Table 1), interaction of chitosan with amino acids Phe249, Glu247 and Asp318 (2-D interaction in Fig. S2B†) of free CGTase G1 predicted to form an ester bond and these results were supported by the presence of C=O stretch peaks at 1643 cm<sup>-1</sup>, 1060 cm<sup>-1</sup> and 1020 cm<sup>-1</sup> indicating C-C-O and O-C-C stretches in CS-CGTG1-CLEA spectrum. The interaction of chitosan with amino acids His223, Arg365, Trp91 and Ala220 of free enzyme is confirmed by the increase in intensity of peaks in the CS-CGTG1-CLEA at 3286 cm<sup>-1</sup> indicating the N—H and O—H stretch and 1643 cm<sup>-1</sup> indicating C=N and C=O. This finding is similar with Nawawi et al. [28] which reported the presence of C=O and C=N functional group between maltogenic amylase (Mag1) and chitosan in Mag1-CLEA.

### 3.6.5. Morphological analysis of CS-CGTG1-CLEA

Field emission scanning electron microscopy (FESEM) on dried sample of CS-CGTG1-CLEA with various magnifications were illustrated in Fig. S9†. The structure of CLEA under an electron microscope can be classified into two types; type 1 aggregate form a ball-like structure, has a diameter around 1  $\mu$ m while type 2 aggregates form a less defined and more random aggregation which is usually smaller with a diameter around 0.1  $\mu$ m [21]. FESEM images (Fig. S9†) revealed that CS-CGTG1-CLEA exhibited a type 1 aggregates with diameter of 2.2  $\pm$  1.3  $\mu$ m. This finding was supported by chitosan-CLEAs of Mag1 [28] and laccase [58] that showed a similar type of structure. Although a smaller size of CLEA (type 2) is expected to have a high surface/volume ratio that helps the diffusion of substrate into the active site, however, based on the kinetic performances of CS-CGTG1-CLEA (Table 3), it possessed about the same catalytic efficiency to free enzyme which discarded the substrate diffusion limitation. Moreover, the smaller size of CLEA will introduce a large pressure drop over the column in continuous operation [20] hence, larger size of CLEAs is more beneficial in this case. Compromise between size and good activity is necessary for large scale applications, in these instance CS-CGTG1-CLEA is more beneficial for large scale applications.

### 3.6.6. Cyclodextrin production and reusability analysis

Cyclodextrin production by free and immobilized CGTase G1 and reusability of CS-CGTG1-CLEA were analyzed using high performance liquid chromatography equipped with a refractive index detector. CGTase G1 produced approximately 80% of  $\beta$ -CD and 20%  $\gamma$ -CD when reacted with starch within 1 to 4 h reaction [46]. The amounts of CDs produced were quantified by the equation based on standard curve plotted using standard  $\beta$ - and  $\gamma$ -CD purchased from the manufacturer (Fig. S10†).

Fig. 7A and B shows the 3 h reaction course in the production of CDs for free and immobilized CGTase G1 while Fig. 7C shows the reusability of CS-CGTG1-CLEA. Immobilized CGTase G1 and free enzyme produced maximum concentration of CDs at 2 h reaction. It was observed that CS-

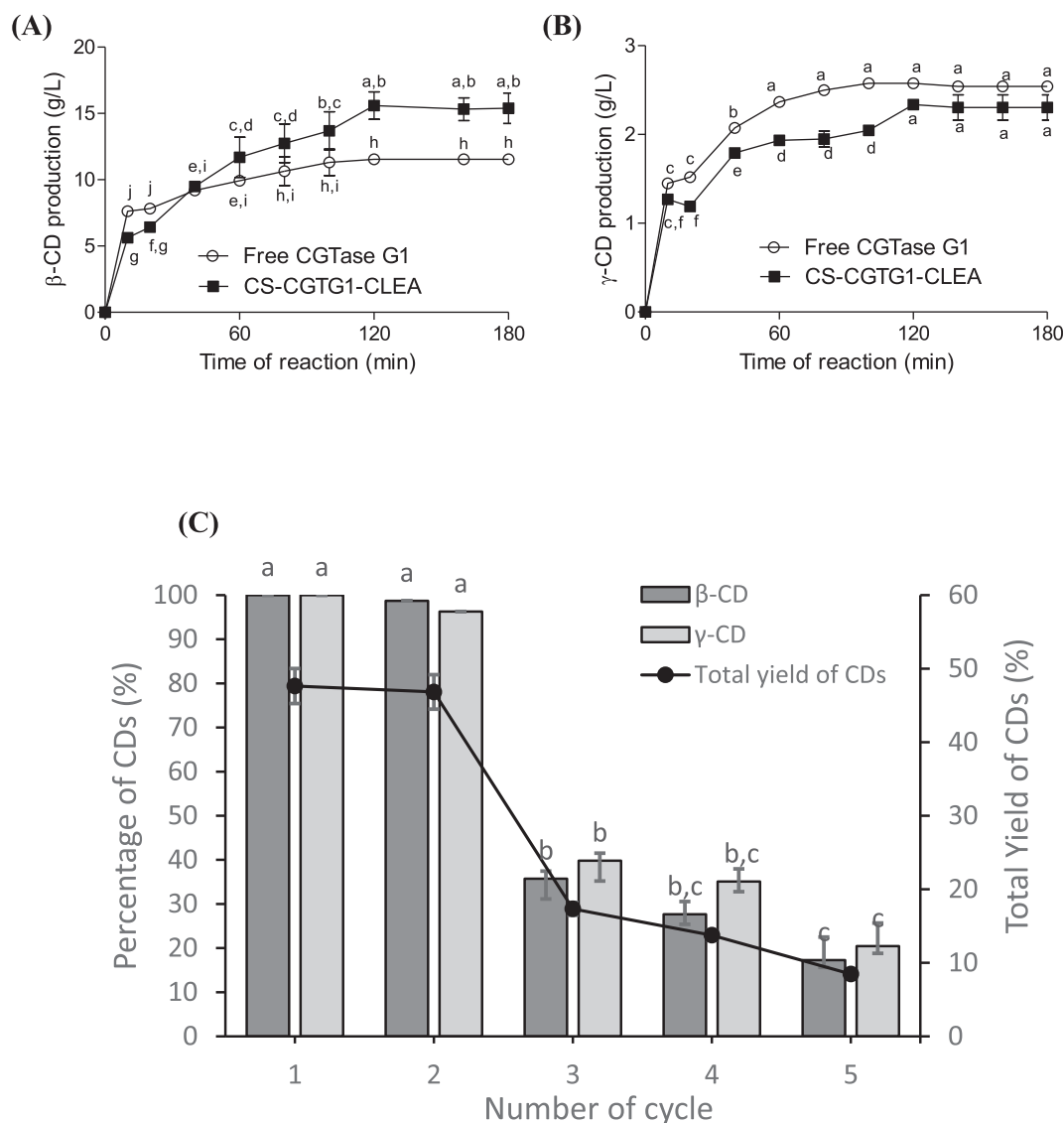


**Fig. 7.** Production of (A)  $\beta$ -CD and (B)  $\gamma$ -CD at 60 °C, pH 6 for 3 h, catalyze by free CGTase G1 and CS-CGTG1-CLEA (25 U/ g starch of 100 mL 4%, w/v soluble starch) (C) Reusability of CS-CGTG1-CLEA in cyclodextrin production at 60 °C, pH 6 using enzyme loading 25 U/ g in 100 mL 4%, w/v soluble starch as a substrate. Each cycle takes 2 h reaction. All experiments were performed in triplicate and the error bar represent the standard deviation error in each of readings. Mean values with the significant differences appear by distinct letters when  $P < 0.05$  by the ANOVA Tukey test.

CGTG1-CLEA (Fig. 7A) produced higher amount of  $\beta$ -CD ( $15.92 \pm 1.5$  g/L) at 2 h reaction compared to free enzyme ( $11.53 \pm 0.5$  g/L) under optimal temperature and pH conditions. Whereas, both free and CS-CGTG1-CLEA (Fig. 7B) permitted around the same amount of  $\gamma$ -CD ( $2.54 \pm 0.3$  g/L and  $2.34 \pm 0.5$  g/L) at 2 h reaction respectively. The total CDs production of CS-CGTG1-CLEA increased by 33% compared to free enzyme. The percentage ratio of  $\beta$ - and  $\gamma$ -CD for immobilized CGTase G1 (86:14) slightly changed compared to free enzyme (83:17) showing that the immobilization might have altered the product specificity.

The reusability of CS-CGTG1-CLEA was evaluated in five cycles each of 2 h reaction under optimal temperature and pH conditions (Fig. 7B). CS-CGTG1-CLEA maintained its activity and yielded 46.8% of total CDs at second cycle from 47.6% total CDs (first cycle). The total CDs decreased during the third cycle (17.3%) and continued to drop during the fourth and fifth cycle (13.8% and 8.5% respectively). The yield of  $\beta$ -CD decreased to 82.7% of the initial yield, while the decrease of  $\gamma$ -CD was 79.5% of the initial productions. This may be due to the instability of chitosan with CGTase G1, which was also predicted earlier from the

RMSD analysis (Fig. 1A). CGTase G1-chitosan complex portrayed high RMSD values indicating low stability over time. The data shown in Fig. 4C also supports this hypothesis as enzyme loss in the washing solution increased over time as chitosan was cross-linked. It is also possible that the washing step in every cycle contributes to a decrease in catalytic efficiency.

The properties of reaction course for the production of CDs and operational stability of reported immobilized CGTase on solid supports and CGTase-CLEAs were compared and are summarized in Table 4. Rakmai and Cheirsilp [14] immobilized CGTase from *Bacillus* sp. C26. in mixed gel beads by entrapment with 90% activity recovery. They reported the  $\beta$ -CD production in an integrated continuous stirred tank reactor and packed-bed reactor performed for 96 h. Using soluble starch at 4%, pH 7 and 50 °C maximum yield of 10.6 g/L  $\beta$ -CD was reached at 60 h before it reduced to 6.38 g/L at 96 h. Schöffer et al. [13] reported the immobilization of a commercial CGTase from *Thermoanaerobacter* sp. on glutaraldehyde pre activated silica and its use to produce CDs in batch and continuous reactions. This immobilization however displayed a poor activity recovery (5.37%) and when the reactor was filled with 1

**Table 4**  
Properties of CGTase immobilized on different supports/CGTase-CLEA for cyclodextrins (CDs) production.

*Support/**cross-linker	Source of CGTase	Optimum pH	Optimum temperature (°C)	Maximum yield of CDs	Activity of immobilized enzyme (U/g-support)/ Activity recovery (%)	Reusability studies (% of initial activity retained after cycles)	Ref
*Mixed alginate-gelatin gel beads	<i>Bacillus</i> sp. C26.	7	50	10.6 g/L (β-CD)	10.5/90	n.r	[14]
*Glutaraldehyde pre activated silica	<i>Thermoanaerobacter</i> sp. (Toruzyme®)	8	70	4.3 mg/mL (α-CD) 4.9 mg/mL (β-CD)	10,173/5.37	n.r	[13]
*Cudlan <sup>a</sup> and *vegetable sponge <sup>b</sup>	<i>Bacillus firmus</i> strain 37	8	50	<sup>a</sup> 3.8 ± 0.2 mmol/L (β-CD) <sup>b</sup> 0.42 ± 0.05 mmol/L (β-CD)	<sup>a</sup> n.r/45 <sup>b</sup> n.r/30	<sup>a</sup> 6.5 ± 0.3 <sup>b</sup> n.d	[72]
*Controlled pore silica	<i>Thermoanaerobacter</i> sp. (Toruzyme®)	6	65	26.29 mmol/L (α-CD) 23.10 mmol/L (β-CD)	n.r/89.63	3.89	[15]
**Dialdehyde starch	<i>Thermoanaerobacter</i> sp. (Toruzyme®)	6	50	2.7 g/L (α-CD) 4.0 g/L (β-CD) 1.8 g/L (γ-CD)	-/24	34.6	[24]
**chitosan	<i>Bacillus</i> sp. G1	6	60	15.92 ± 1.5 g/L (β-CD) 2.34 ± 0.5 g/L (γ-CD)	-/90.2 ± 0.45	8.5	This study

n.r = not reported, n.d = not detected, \*type of support, \*\*type of cross-linker.

g of immobilized CGTase with 4% (w/v) soluble starch as a substrate, the production of α- and β-CD, reaching to only 4.3 and 4.9 mg/mL, respectively at 6.72 min of reaction (pH 8, 70 °C). Low activity recovery in this report could be caused by the mesoporous nature of the silica used, preventing the substrate from accessing the active sites.

On the other hand, Fenelon et al. [72] reported the immobilization of CGTase from *Bacillus firmus* strain 37 on two natural supports curdlan and vegetables sponge (*Luffa cylindrica*), both of which are composed of polymeric chains of glucose that contain an abundance of free hydroxyl groups. Both immobilized CGTases portrayed 45% and 30% activity recovery, respectively. Four repetitive batches of immobilized curdlan and vegetable sponge were performed using 5% corn starch in the presence of 10% ethanol for 12 h, pH 8 at 50 °C for CDs production evaluation. The concentration of β-CD reached 8.9 mmol/L (curdlan) and 1.27 mmol/L (vegetables sponge) at the end of first batch however, yield of β-CD decreased intensively were observed in the following batches. Immobilized CGTase on curdlan retained 6.5 ± 0.3% of its initial β-CD activity, but the presence of β-CD was no longer detectable in the reaction medium for CGTase immobilized on vegetables sponges after fourth batches. Gimenez et al. [15] applied the immobilization of commercial CGTase from *Thermoanaerobacter* sp. into controlled pore silica by surface anchoring and covalent bonding method for the production of CDs. Immobilization of CGTase into pore silica by anchoring method possessed higher activity recovery (89.63%) compared to covalent binding (48.44%). Immobilized CGTase by anchoring method in this study efficiently produced 18.15% higher total CDs with maximal yield of 26.29 mmol/L (α-CD) and 23.10 mmol/L (β-CD) compared to free enzyme at the end of 24 h reaction using 10% cassava starch in the presence of 10% ethanol at 65 °C, pH 6. However, poor reusability was observed with a decline in 61.51% of total CDs in the second cycle and only retained 3.89% from its initial CDs production after five consecutive cycles tested. A report by Rojas et al. [24] showed that *Thermoanaerobacter* sp. CGTase-CLEA using dialdehyde starch as a cross-linker produced maximum yield of β- and γ-CD (4.0 and 1.8 g/L, respectively) after 3 h reaction from 2% starch at 50 °C, pH 6. The operational stability of CGTase-CLEA in this study displayed a 66% β-CD decrease of the initial ones, while the γ-CD decreased to 94% of the initial productions in five reaction cycles of 3 h at 50 °C (with total cumulative CDs was 37.1 g/L).

While, different sources of CGTase produce different CDs ratio, in this report, CS-CGTG1-CLEA from *Bacillus lehensis* G1 managed to

produce higher amount of β-CD at lower time of reaction compared with immobilized CGTase in mixed alginate-gelatin gel beads [14] and 2 times higher amount of β-CD at lower time of reaction compared to the previous CGTase-CLEA [24] (Table 4). β-CD is the most accessible and generally the most useful compared to α- and γ-CD in industrial applications [3,6–8] thus showing the advantage of CS-CGTG1-CLEA that produced higher amount of β-CD. However, despite the decreased of a β-CD in this study is more pronounced from the initial ones, the total cumulative yield of CDs (β-CD and γ-CD) is much higher (52.62 g/L) than previous CGTase-CLEA (23.81 g/L) [24] with a difference of 120.9% after the same number of cycles. It was observed that studied done by Gimenez et al. [15] which immobilized the CGTase in controlled pore silica also portrayed a poor reusability (Table 4) hence showed that the operational stability of CS-CGTG-CLEA in this study is still promising and better for production of CDs compared to previous study.

#### 4. Conclusions

In summary, cross-linked cyclodextrin glucanotransferase aggregates immobilization has been developed using a combination of computational tools to produce CDs from starch. CGTase G1 with chitosan complex displayed the highest binding affinity, high RMSF values attributed to its flexibility and largest radius of gyration among other cross-linkers tested by docking and molecular dynamic (MD) simulation analyses. Following this, CGTase G1 cross-linked with chitosan (CS-CGTG1-CLEA) gave the highest activity recovery (84.6 ± 0.26%) when CLEA was developed among six other cross-linkers tested under optimized screening conditions (0.01% (v/v) concentration of cross-linker and cross-linked for 1 h). CS-CGTG1-CLEA was further optimized to achieve 90.2 ± 0.45% activity recovery when the chitosan concentration used was 0.15% (v/v) and crosslinked for 1 h. Immobilized chitosan-CGTase G1-CLEA displayed the same characteristic with free enzyme in terms of its optimum temperature, pH and kinetic performances however showed a greater thermostability, longer half-life, yielded a higher total CDs by 33% and displayed a promising operational stability to produce CDs (total cumulative of CDs of 52.62 g/L after 5 cycles for 2 h reactions).

Different types of cross-linkers with different functional groups was observed to possess different characteristic (binding energy, RMSD, RMSF and radius of gyration) in its interaction with CGTase G1 amino

acid residues. Chitosan with abundance of hydroxy functional group showed the strongest binding affinity due to the existence of the highest number of hydrogen bonds interacted with eight residues of CGTase G1. This study provides new insight into the molecular interaction between cross-linker with enzyme surface residue whereby the corroboration of *in-silico* analysis with the experimental data here may prove that computational-based approaches can be used as a guide for cross-linker screening and eventually be adapted to minimize the laborious step in selecting the cross-linker based on different enzyme to produce their most active CLEA in the future.

#### CRedit authorship contribution statement

**Nashriq Jailani:** Methodology; Investigation; Formal analysis; Validation; Writing- Original draft; Writing – review & editing.

**Nardiah Rizwana Jaafar:** Methodology; Validation; Writing- Original draft; Writing – review & editing.

**Suhaily Suhaimi:** Methodology; Investigation.

**Mukram Mohamed Mackeen:** Conceptualization; Supervision.

**Farah Diba Abu Bakar:** Conceptualization; Funding acquisition; Validation; Supervision.

**Rosli Md Illias:** Conceptualization; Funding acquisition; Validation; Project administration; Supervision; Validation; Writing-Original draft; Writing – review & editing.

#### Data availability

Data will be made available on request.

#### Acknowledgement

This work was supported by the Ministry of Higher Education, Malaysia under Grant FRGS (FRGS/1/2018/STG05/UTM/01/1). The authors thank the School of Chemical and Energy Engineering, Faculty of Engineering at Universiti Teknologi Malaysia for access to their facilities and technical support.

#### Appendix A. Supplementary data

Supplementary data to this article can be found online at <https://doi.org/10.1016/j.ijbiomac.2022.05.170>.

#### References

- [1] A. Tonkova, Bacterial cyclodextrin glucanotransferase, *Enzym. Microb. Technol.* 22 (1998) 678–686.
- [2] V. Bautista, J. Esclapez, F. Pérez-Pomares, R.M. Martínez-Espinoza, M. Camacho, M.J. Bonete, Cyclodextrin glycosyltransferase: a key enzyme in the assimilation of starch by the halophilic archaeon *Haloferax mediterranei*, *Extremophiles* 16 (2012) 147–159.
- [3] B. Cheirsilp, J. Rakmai, Inclusion complex formation of cyclodextrin with its guest and their applications, *Biol. Eng. Med.* 2 (2017) 1–6.
- [4] Y. Chen, Y. Liu, Cyclodextrin-based bioactive supramolecular assemblies, *Chem. Soc. Rev.* 39 (2010) 495–505.
- [5] J. Wankar, N.G. Kotla, S. Gera, S. Rasala, A. Pandit, Y.A. Rochev, Recent advances in host-guest self-assembled cyclodextrin carriers: implications for responsive drug delivery and biomedical engineering, *Adv. Funct. Mater.* 30 (2020), 1909049.
- [6] G. Astray, J.C. Mejuto, J. Simal-Gandara, Latest developments in the application of cyclodextrin host-guest complexes in beverage technology processes, *Food Hydrocoll.* 106 (2020), 105882.
- [7] S. Qie, Y. Hao, Z. Liu, J. Wang, J. Xi, Advances in cyclodextrin polymers and their applications in biomedicine, *Acta Chim. Sin.* 78 (2020) 232–244.
- [8] M. Rehan, S.A. Mahmoud, H.M. Mashaly, B.M. Youssef,  $\beta$ -Cyclodextrin assisted simultaneous preparation and dyeing acid dyes onto cotton fabric, *React. Funct. Polym.* 151 (2020), 104573.
- [9] J. Lee, S. Park, Review of the usability of cyclodextrin as a cosmetic ingredient, *Asian J. Beauty Cosmetol.* 17 (2019) 545–553.
- [10] M. Bilal, H.M.N. Iqbal, Chemical, physical, and biological coordination: an interplay between materials and enzymes as potential platforms for immobilization, *Coord. Chem. Rev.* 388 (2019) 1–23.
- [11] M. Bilal, H.M.N. Iqbal, S. Guo, H. Hu, W. Wang, X. Zhang, State-of-the-art protein engineering approaches using biological macromolecules: a review from immobilization to implementation view point, *Int. J. Biol. Macromol.* 108 (2018) 893–901.
- [12] M. Bilal, Z. Jing, Y. Zhao, H.M.N. Iqbal, Immobilization of fungal laccase on glutaraldehyde cross-linked chitosan beads and its bio-catalytic potential to degrade bisphenol A, *Biocatal. Agric. Biotechnol.* 19 (2019), 101174.
- [13] J. Da, N. Schöffner, C.R. Matte, D.S. Charqueiro, E.W. de Menezes, T.M.H. Costa, E. V. Benvenuti, R.C. Rodrigues, P.F. Hertz, Effects of immobilization, pH and reaction time in the modulation of  $\alpha$ -,  $\beta$ - or  $\gamma$ -cyclodextrins production by cyclodextrin glycosyltransferase: batch and continuous process, *Carbohydr. Polym.* 169 (2017) 41–49.
- [14] J. Rakmai, B. Cheirsilp, Continuous production of  $\beta$ -cyclodextrin by cyclodextrin glycosyltransferase immobilized in mixed gel beads: comparative study in continuous stirred tank reactor and packed bed reactor, *Biochem. Eng. J.* 105 (2016) 107–113.
- [15] G.G. Gimenez, R.M. Silva, C.P. Francisco, J.H. Dantas, H.M. de Souza, G. Matioli, F. Dos, S. Rando, Immobilization of commercial cyclomaltodextrin glucanotransferase into controlled pore silica by the anchorage method and covalent bonding, *Process Biochem.* 85 (2019) 68–77.
- [16] S. Liu, M. Bilal, K. Rizwan, I. Gul, T. Rasheed, H.M.N. Iqbal, Smart chemistry of enzyme immobilization using various support matrices – a review, *Int. J. Biol. Macromol.* 190 (2021) 396–408.
- [17] M. Bilal, M. Asgher, H. Cheng, Y. Yan, H.M.N. Iqbal, Multi-point enzyme immobilization, surface chemistry, and novel platforms: a paradigm shift in biocatalyst design, *Crit. Rev. Biotechnol.* 39 (2019) 202–219.
- [18] M. Bilal, S.A. Qamar, S.S. Ashraf, S. Rodriguez-Couto, H.M.N. Iqbal, Robust nanocarriers to engineer nanobiocatalysts for bioprocessing applications, *Adv. Colloid Interf. Sci.* 293 (2021).
- [19] M. Bilal, T. Anh Nguyen, H.M.N. Iqbal, Multifunctional carbon nanotubes and their derived nano-constructs for enzyme immobilization – a paradigm shift in biocatalyst design, *Coord. Chem. Rev.* 422 (2020), 213475.
- [20] R. Sheldon, CLEAs, combi-CLEAs and ‘smart’ magnetic CLEAs: biocatalysis in a bio-based economy, *Catalysts* 9 (2019) 261.
- [21] M.T. De Martino, F. Tonin, N.A. Yewdall, M. Abdelghani, D.S. Williams, U. Hanefeld, F.P.J.T. Rutjes, L.K.E.A. Abdelmohsen, J.C.M. Van Hest, Compartmentalized cross-linked enzymatic nano-aggregates (c-CLE n A) for efficient in-flow biocatalysis, *Chem. Sci.* 11 (2020) 2765–2769.
- [22] S. Velasco-Lozano, F. López-Gallego, J.C. Mateos-Díaz, E. Favela-Torres, Cross-linked enzyme aggregates (CLEA) in enzyme improvement – a review, *Biocatalysis* 1 (2016) 166–177.
- [23] O. Barbosa, C. Ortiz, Á. Berenguer-Murcia, R. Torres, R.C. Rodrigues, R. Fernandez-Lafuente, Glutaraldehyde in bio-catalysts design: a useful crosslinker and a versatile tool in enzyme immobilization, *RSC Adv.* 4 (2014) 1583–1600.
- [24] M. Rojas, M. Amaral-Fonseca, G. Zanin, R. Fernandez-Lafuente, R. Giordano, P. Tardioli, Preparation of crosslinked enzyme aggregates of a thermostable cyclodextrin glucosyltransferase from thermoanaerobacter spCritical Effect of the Crosslinking Agent, *Catalysts* 9 (2019) 120.
- [25] J. Zhang, M. Li, H. Mao, Cross-linked enzyme aggregates of recombinant cyclodextrin glycosyltransferase for high-purity  $\beta$ -cyclodextrin production, *J. Chem. Technol. Biotechnol.* 94 (2019) 1528–1533.
- [26] A. Wang, F. Zhang, F. Chen, M. Wang, H. Li, Z. Zeng, T. Xie, Z. Chen, A facile technique to prepare cross-linked enzyme aggregates using p-benzoquinone as cross-linking agent, *Korean J. Chem. Eng.* 28 (2011) 1090–1095.
- [27] H. Ayhan, F. Ayhan, A. Gülsu, Highly biocompatible enzyme aggregates crosslinked by L-lysine, <article-title><sb:contribution><sb:issue><sb:series><sb:title>J. Biochem.</sb:title></sb:series></sb:issue></sb:host></article-title><sb: host><sb:issue><sb:series><sb:title></sb:title></sb:series></sb:issue></sb: host> 37 (2012) 14–20.
- [28] N.N. Nawawi, Z. Hashim, N.H.A. Manas, N.I.W. Azelee, R.M. Illias, A porous-cross linked enzyme aggregates of maltogenic amylase from *Bacillus lehensis G1*: robust biocatalyst with improved stability and substrate diffusion, *Int. J. Biol. Macromol.* 148 (2020) 1222–1231.
- [29] J. Fan, A. Fu, L. Zhang, Progress in molecular docking, *Quant. Biol.* 7 (2019) 83–89.
- [30] A.A.T. Naqvi, T. Mohammad, G.M. Hasan, M.I. Hassan, Advancements in docking and molecular dynamics simulations towards ligand-receptor interactions and structure-function relationships, *Curr. Top. Med. Chem.* 18 (2019) 1755–1768.
- [31] V. Salmasso, S. Moro, Bridging molecular docking to molecular dynamics in exploring ligand-protein recognition process: an overview, *Front. Pharmacol.* 9 (2018) 1–16.
- [32] C. Li, Z. Lu, M. Wang, S. Chen, L. Han, W. Han, A possible mechanism of graphene oxide to enhance thermostability of D-psicose 3-epimerase revealed by molecular dynamics simulations, *Int. J. Mol. Sci.* 22 (2021) 10813.
- [33] X. Sun, Z. Feng, T. Hou, Y. Li, Mechanism of graphene oxide as an enzyme inhibitor from molecular dynamics simulations, *ACS Appl. Mater. Interfaces* 6 (2014) 7153–7163.
- [34] M. Calvaresi, S. Hoefinger, F. Zerbetto, Probing the structure of lysozyme-carbon-nanotube hybrids with molecular dynamics, *Chem. Eur. J.* 18 (2012) 4308–4313.
- [35] H. Zhou, Y. Qu, C. Kong, D. Li, E. Shen, Q. Ma, X. Zhang, J. Wang, J. Zhou, Catalytic performance and molecular dynamic simulation of immobilized CC bond hydrolase based on carbon nanotube matrix, *Colloids Surf. B Biointerfaces* 116 (2014) 365–371.
- [36] K.M. Goh, N.M. Mahadi, O. Hassan, R.N. Zaliha, R.A. Rahman, R.M. Illias, Molecular modeling of a predominant  $\beta$ -CGTase G1 and analysis of ionic interaction in CGTase, *Biotechnology* 7 (2008) 418–429.

- [37] B. Hess, C. Kutzner, D. van der Spoel, E. Lindahl, GROMACS 4: algorithms for highly efficient, load-balanced, and scalable molecular simulation, *J. Chem. Theory Comput.* 4 (2008) 435–447.
- [38] S. Kim, J. Chen, T. Cheng, A. Gindulyte, J. He, S. He, Q. Li, B.A. Shoemaker, P. A. Thiessen, B. Yu, L. Zaslavsky, J. Zhang, E.E. Bolton, PubChem in 2021: new data content and improved web interfaces, *Nucleic Acids Res.* 49 (2021) D1388–D1395.
- [39] O. Trott, A.J. Olson, AutoDock Vina: improving the speed and accuracy of docking with a new scoring function, efficient optimization, and multithreading, *J. Comput. Chem.* 31 (2010) 455–461.
- [40] T. Darden, D. York, L. Pedersen, Particle mesh Ewald: an  $N^{-1}$  method for Ewald sums in large systems, *J. Chem. Phys.* 98 (1993) 10089–10092.
- [41] W.L. DeLano, The PyMOL Molecular Graphics System, Version 2.3, Schrödinger LLC, 2020.
- [42] R.A. Laskowski, M.B. Swindells, LigPlot+: multiple ligand-protein interaction diagrams for drug discovery, *J. Chem. Inf. Model.* 51 (2011) 2778–2786.
- [43] R. Illias, S. Tien, R. Rahman, N. Rashid, W. Yusoff, A. Hamid, O. Hassan, K. Kamaruddin, Application of factorial design to study the effects of temperature, initial pH and agitation on the production of cyclodextrin glucanotransferase from alkalophilic *Bacillus* sp. G1, *Sci. Asia* 29 (2003) 135–140.
- [44] H.L. Ling, Z. Rahmat, A.M.A. Murad, N.M. Mahadi, R.M. Illias, Proteome-based identification of signal peptides for improved secretion of recombinant cyclomaltodextrin glucanotransferase in *Escherichia coli*, *Process Biochem.* 61 (2017) 47–55.
- [45] T. Kaneko, T. Kato, N. Nakamura, K. Horikoshi, Spectrophotometric determination of cyclization activity of BETA-cyclodextrin-forming cyclomaltodextrin glucanotransferase, *J. Jpn. Soc. Starch Sci.* 34 (1987) 45–48.
- [46] R.M. Ong, K.M. Goh, N.M. Mahadi, O. Hassan, R.N.Z.R.A. Rahman, R.M. Illias, Cloning, extracellular expression and characterization of a predominant  $\beta$ -CGTase from *Bacillus* sp. G1 in *E. coli*, *J. Ind. Microbiol. Biotechnol.* 35 (2008) 1705–1714.
- [47] J. Yu, P.R. Chang, X. Ma, The preparation and properties of dialdehyde starch and thermoplastic dialdehyde starch, *Carbohydr. Polym.* 79 (2010) 296–300.
- [48] S. Veelaert, D. De Wit, K.F. Gotlieb, R. Verhé, Chemical and physical transitions of periodate oxidized potato starch in water, *Carbohydr. Polym.* 33 (1997) 153–162.
- [49] M. Tummalapalli, B. Gupta, A UV-vis spectrophotometric method for the estimation of aldehyde groups in periodate-oxidized polysaccharides using 2,4-dinitrophenyl hydrazine, *J. Carbohydr. Chem.* 34 (2015) 338–348.
- [50] I. Santamaría-Holek, A. Pérez-Madrid, Eyring equation and fluctuation-dissipation far away from equilibrium, *J. Chem. Phys.* 153 (2020), 244116.
- [51] H. Lineweaver, D. Burk, The determination of enzyme dissociation constants, *J. Am. Chem. Soc.* 56 (1934) 658–666.
- [52] M.A. Strege, S. Huang, D.S. Rislely, Quantitative determination of beta-cyclodextrin in a powder insulin formulation for nasal delivery using hydrophilic interaction chromatography with evaporative light scattering detection, *J. Liq. Chromatogr. Relat. Technol.* 42 (2019) 74–78.
- [53] H. Jalily Hasani, K. Barakat, Homology modeling: an overview of fundamentals and tools, *Int. Rev. Model. Simul.* 10 (2017) 129.
- [54] B. Webb, A. Sali, Comparative protein structure modeling using MODELLER, *Curr. Protoc. Bioinforma.* 54 (2016) 5.6.1–5.6.37.
- [55] B. Banaganapalli, F.A. Morad, M. Khan, C.S. Kumar, R. Elango, Z. Awan, N. A. Shaik, Molecular docking, in: I. Vol (Ed.), *Essentials Bioinformatics*, Springer International Publishing, Cham, 2019, pp. 335–353.
- [56] S.A. Hollingsworth, R.O. Dror, Molecular dynamics simulation for all, *Neuron* 99 (2018) 1129–1143.
- [57] R.A. Sheldon, S. van Pelt, Enzyme immobilisation in biocatalysis: why, what and how, *Chem. Soc. Rev.* 42 (2013) 6223–6235.
- [58] A. Arsenault, H. Cabana, J.P. Jones, Laccase-based CLEAs: chitosan as a novel cross-linking agent, *Enzyme Res.* 2011 (2011).
- [59] S.S. Nadar, A.B. Muley, M.R. Ladole, P.U. Joshi, Macromolecular cross-linked enzyme aggregates (M-CLEAs) of  $\alpha$ -amylase, *Int. J. Biol. Macromol.* 84 (2016) 69–78.
- [60] M.K.H. Abdull Wahab, H.A. El-Enshasy, F.D.A. Bakar, A.M.A. Murad, J.M. Jahim, R. M. Illias, Improvement of cross-linking and stability on cross-linked enzyme aggregate (CLEA)-xylanase by protein surface engineering, *Process Biochem.* 86 (2019) 40–49.
- [61] R.A. Sheldon, S. van Pelt, S. Kanbak-Aksu, J.A. Rasmussen, M.H.A. Janssen, Cross-linked enzyme aggregates (CLEAs) in organic synthesis, *Aldrichimica Acta* 46 (2013) 81–93.
- [62] I. Migneault, C. Dartiguenave, M.J. Bertrand, K.C. Waldron, Glutaraldehyde: behavior in aqueous solution, reaction with proteins, and application to enzyme crosslinking, *Biotechniques* 37 (2004) 790–802.
- [63] L. Cao, F. Van Rantwijk, R.A. Sheldon, Cross-linked enzyme aggregates: a simple and effective method for the immobilization of penicillin acylase, *Org. Lett.* 2 (2000) 1361–1364.
- [64] M.L. Verma, S. Kumar, A. Das, J.S. Randhawa, M. Chamundeswari, Chitin and chitosan-based support materials for enzyme immobilization and biotechnological applications, *Environ. Chem. Lett.* 18 (2020) 315–323.
- [65] N.H. Abd Rahman, N.R. Jaafar, A.M. Abdul Murad, F.D. Abu Bakar, N.A. Shamsul Annuar, R.M. Illias, Novel cross-linked enzyme aggregates of levanase from *Bacillus* lehensis G1 for short-chain fructooligosaccharides synthesis: Developmental, physicochemical, kinetic and thermodynamic properties, *Int. J. Biol. Macromol.* 159 (2020) 577–589.
- [66] L. Wilson, L. Betancor, G. Fernández-Lorente, M. Fuentes, A. Hidalgo, J.M. Guisán, B.C.C. Pessela, R. Fernández-Lafuente, Cross-linked aggregates of multimeric enzymes: a simple and efficient methodology to stabilize their quaternary structure, *Biomacromolecules* 5 (2004) 814–817.
- [67] A. Basso, S. Serban, Industrial applications of immobilized enzymes—a review, *Mol. Catal.* 479 (2019), 110607.
- [68] S. Rehman, H.N. Bhatti, M. Bilal, M. Asgher, Cross-linked enzyme aggregates (CLEAs) of *Penicillium notatum* lipase enzyme with improved activity, stability and reusability characteristics, *Int. J. Biol. Macromol.* 91 (2016) 1161–1169.
- [69] E.A. Karam, W.A. Abdel Wahab, S.A.A. Saleh, M.E. Hassan, A.L. Kansoh, M. A. Esawy, Production, immobilization and thermodynamic studies of free and immobilized *Aspergillus awamori* amylase, *Int. J. Biol. Macromol.* 102 (2017) 694–703.
- [70] S.H. Mansour, A.M. Abdel-Fattah, M.A. Esawy, E.F. Ahmed, A.A. Haroun, M. A. Hussein, N.M. Hassanien, H.M. Khater, Immobilization, thermodynamic studies and application of chitinase enzyme from *Penicillium chrysogenum*, Egypt, *J. Aquat. Biol. Fish.* 23 (2019) 527–544.
- [71] M.A. Abdel-Naby, A. Fouad, R.M. Reyad, Catalytic and thermodynamic properties of immobilized *Bacillus amyloliquefaciens* cyclodextrin glucosyltransferase on different carriers, *J. Mol. Catal. B Enzym.* 116 (2015) 140–147.
- [72] V.C. Felon, J.H. Miyoshi, C.S. Mangolim, A.S. Noce, L.N. Koga, G. Matioli, Different strategies for cyclodextrin production: ultrafiltration systems, CGTase immobilization and use of a complexing agent, *Carbohydr. Polym.* 192 (2018) 19–27.